

ENTANGLEMENT OF RESONANTLY COUPLED FIELD MODES IN CAVITIES WITH VIBRATING BOUNDARIES

M. A. Andreata, A. V. Dodonov, and V. V. Dodonov¹

*Departamento de Física, Universidade Federal de São Carlos,
Via Washington Luiz, km 235, 13565-905 São Carlos, SP, Brasil*
e-mail: vdodonov@df.ufscar.br

Abstract

We study time dependence of various measures of entanglement (covariance entanglement coefficient, purity entanglement coefficient, normalized distance coefficient, entropy coefficients) between resonantly coupled modes of the electromagnetic field in ideal cavities with oscillating boundaries. Two types of cavities are considered — a three-dimensional cavity possessing eigenfrequencies $\omega_3 = 3\omega_1$, whose wall oscillates at the frequency $\omega_w = 2\omega_1$, and a one-dimensional (Fabry–Perot) cavity with an equidistant spectrum $\omega_n = n\omega_1$ where the distance between perfect mirrors oscillates at the frequencies ω_1 and $2\omega_1$. The behavior of entanglement measures in these cases turns out to be completely different, although all three coefficients demonstrate qualitatively similar time dependences in each case (except some specific situations where the covariance entanglement coefficient based on traces of covariance submatrices seems to be essentially more sensitive to entanglement than other measures, which are based on determinants of covariance submatrices). Different initial states of the field, namely, vacuum, squeezed vacuum, thermal, Fock, and even/odd coherent states, are considered.

Keywords: dynamical Casimir effect, vibrating boundary, parametric resonance, coupled modes, entanglement, quantum purity, entropy, distance, covariances, Fock states, Gaussian states, even/odd coherent states, squeezed states, thermal states.

1. Introduction

During the past decade it was recognized that the concept of entanglement introduced by Schrödinger in 1935 [1, 2] is not only one of the most profound in quantum mechanics (as was shown in the same year by Einstein, Podolsky, and Rosen in their famous paper [3], albeit without using explicitly this word) but is also crucial for many promising new applications such as quantum cryptography, quantum communication and teleportation, quantum computing, etc. This explains the burst of interest in various problems connected with this concept observed in the past few years. One of such problems is the search for quantitative measures of entanglement.

In most cases, measures based on different kinds of entropies have been considered [4–9]. For example, if the total system, consisting of parts 1 and 2, is described by means of the statistical operator $\hat{\rho}_0$, then the entanglement measure is frequently expressed in terms of the total and “partial” entropies as the “index of correlation” [4]

$$I_c = S_1 + S_2 - S_0, \quad S_k = -\text{Tr}_k \hat{\rho}_k \ln \hat{\rho}_k, \quad (1)$$

¹On leave from the P. N. Lebedev Physical Institute and Moscow Institute of Physics and Technology, Russia

where the reduced statistical operator is defined, e.g., as

$$\hat{\rho}_1 = \text{Tr}_2 \hat{\rho}_0.$$

For the total pure states, formula (1) is reduced to

$$I_c = 2S_1 = 2S_2.$$

However, despite many advantages, measures such as (1) are not very convenient from the practical point of view — in order to calculate them, one has to diagonalize the reduced statistical operators and this is a rather difficult problem in the generic case, especially for infinite-dimensional Hilbert spaces (corresponding to the so-called “continuous variable systems”), except for a few simple special cases. Therefore, many authors looked for other measures that could be calculated more easily.

In our paper, we consider several families of simplified measures. The first one is based on the notion of quantum purity

$$\mu = \text{Tr} \hat{\rho}^2$$

or “linear entropy”

$$S^L = 1 - \mu.$$

Different measures containing these quantities were proposed in [7–11]. Measures based on the Hilbert–Schmidt distance between given state and its “disentangled” counterpart were proposed in [12, 13]. On the other hand, even simpler (although nonuniversal) measures of entanglement of continuous variable quantum systems, expressed in terms of the cross-covariances of the quadrature components or the annihilation/creation operators, have recently been introduced in [14, 15]. These measures are discussed in Sec. 2.

One of the numerous possible applications of entanglement measures is a compact quantitative characterization of the evolution of coupled quantum mechanical systems. We started these studies in [14] where two harmonic oscillators with constant frequencies but with the most general time-dependent resonance couplings were considered. The aim of the present paper is to compare different measures in the case where the field modes in a cavity are entangled due to the motion of its boundary (the physical reason of entanglement in this case is the Doppler effect). This case is reduced to models of two or more oscillators with time-dependent frequencies and a specific time-dependent coupling (of the “coordinate–momentum” type).

We consider two types of cavities, starting with a three-dimensional cavity with accidental degeneracy of the spectrum (which happens, e.g., in cubic cavities), when only two modes can occur in resonance with an oscillating wall (Sec. 3). A one-dimensional (Fabry–Perot) cavity is considered in Sec. 4. In this case, all modes are coupled due to the equidistance of the (unperturbed) spectrum of the field eigenfrequencies. It was discovered as far back as in [16] that the field evolution in three- and one-dimensional cavities is qualitatively different. For example, in the 3D case the number of photons in the resonance modes increases with time exponentially, whereas in the 1D case the growth is linear. It was pointed out in [16] that the increase in the number of photons in the 1D cavity is slowed down due to strong intermode interaction, which is equivalent in this case to entanglement. Now we are able to give a quantitative characterization of such an entanglement. The results of our study are discussed in Sec. 5.

2. Purity, Distance, and Covariance Measures of Entanglement

2.1. Purity Entanglement Measure

By analogy with definition (1), the “linear entropy of entanglement” can be defined as

$$\mathcal{L} = S_1^L + S_2^L - S_0^L = 1 + \text{Tr} \hat{\rho}^2 - \text{Tr}_1 \hat{\rho}_1^2 - \text{Tr}_2 \hat{\rho}_2^2. \quad (2)$$

Such a definition appears reasonable if the total system is in a pure quantum state. Then

$$\text{Tr} \hat{\rho}^2 = 1 \quad \text{and} \quad \text{Tr}_1 \hat{\rho}_1^2 = \text{Tr}_2 \hat{\rho}_2^2,$$

so that

$$\mathcal{L} = 2S_1^L = 2S_2^L.$$

As a matter of fact, only this case was considered in the earlier studies [10, 11] where measures of entanglement were identified with the linear entropy of the state of a subsystem or with some equivalent quantities, such as the purity itself, the “participation ratio” $1/\text{Tr}_k \hat{\rho}_k^2$, or the “Renyi entropy”

$$S^R = -\ln (\text{Tr}_k \hat{\rho}_k^2).$$

However, if the state of the total system is a mixed one, then definition (2) leads to some unexpected consequences. Consider, for example, a generic Gaussian two-mode state described by means of the Wigner function (we assume $\hbar = 1$ throughout the paper)

$$W(\mathbf{q}) = |\det(\mathcal{Q})|^{-1/2} \exp \left[-\frac{1}{2} (\mathbf{q} - \langle \mathbf{q} \rangle) \mathcal{Q}^{-1} (\mathbf{q} - \langle \mathbf{q} \rangle) \right], \quad \int W(\mathbf{q}) d\mathbf{q} / (2\pi)^2 = 1, \quad (3)$$

where $\mathbf{q} = (x_1, p_1, x_2, p_2)$, and the symmetrical 4×4 covariance matrix \mathcal{Q} consists of 2×2 blocks

$$\mathcal{Q} = \parallel q_{\alpha\beta} \parallel = \left\| \begin{array}{cc} \mathcal{Q}_{11} & \mathcal{Q}_{12} \\ \mathcal{Q}_{21} & \mathcal{Q}_{22} \end{array} \right\|, \quad \mathcal{Q}_{11} = \tilde{\mathcal{Q}}_{11}, \quad \mathcal{Q}_{22} = \tilde{\mathcal{Q}}_{22}, \quad \mathcal{Q}_{12} = \tilde{\mathcal{Q}}_{21} \quad (4)$$

(a tilde over matrices means matrix transposition). The symmetrical real covariances are defined as

$$q_{\alpha\beta} \equiv \frac{1}{2} (\overline{q_\alpha q_\beta} + \overline{q_\beta q_\alpha}) \equiv \widetilde{q_\alpha q_\beta}, \quad \overline{ab} \equiv \langle \widehat{ab} \rangle - \langle \widehat{a} \rangle \langle \widehat{b} \rangle \quad (5)$$

(in other words, a straight line over the product of two observables means the ordered centralized average value, whereas a wide tilde means the symmetrized centralized average value). Then

$$\mu \equiv \text{Tr} \hat{\rho}^2 = \int [W(\mathbf{q})]^2 \frac{d\mathbf{q}}{(2\pi)^2} q = [\det(2\mathcal{Q})]^{-1/2}. \quad (6)$$

For factorized (disentangled) states,

$$\mathcal{Q}_{12} \equiv 0,$$

therefore,

$$\det \mathcal{Q} = \det \mathcal{Q}_{11} \det \mathcal{Q}_{22} \quad \text{and} \quad \mu = \mu_1 \mu_2,$$

which results in the relations

$$\mathcal{L}_{\text{fact}} = 1 + \mu_1\mu_2 - \mu_1 - \mu_2 = (1 - \mu_1)(1 - \mu_2).$$

Consequently, for mixed states ($\mu < 1$) one can encounter the situation where $\mathcal{L} > 0$ in the absence of any entanglement, if $\mu_1 \neq 1$ and $\mu_2 \neq 1$.

It seems better to use the difference

$$\mathcal{L}_* = \mathcal{L} - \mathcal{L}_{\text{fact}} = \mu - \mu_1\mu_2,$$

but it tends to zero when $\mu \rightarrow 0$. For this reason, we introduce the normalized purity entanglement coefficient

$$\tilde{\mathcal{L}} = 1 - \frac{\mu_1\mu_2}{\mu}. \quad (7)$$

For Gaussian states (3), it can be expressed as

$$\tilde{\mathcal{L}} = 1 - \sqrt{\frac{\det \mathcal{Q}}{\det \mathcal{Q}_{11} \det \mathcal{Q}_{22}}} = 1 - \sqrt{\det \left(E - \mathcal{Q}_{12} \mathcal{Q}_{22}^{-1} \mathcal{Q}_{21} \mathcal{Q}_{11}^{-1} \right)}. \quad (8)$$

The second equality (where E stands for the unit matrix) is obtained with the aid of the known formula for the determinant of a block matrix [17]

$$\det \mathcal{Q} = \det \left(\mathcal{Q}_{11} - \mathcal{Q}_{12} \mathcal{Q}_{22}^{-1} \mathcal{Q}_{21} \right) \det \mathcal{Q}_{22}.$$

In particular, for pure composite states ($\mu = 1$) we have

$$\tilde{\mathcal{L}} = 1 - \mu_1^2 = 1 - \mu_2^2 = \frac{1}{4} \mathcal{L}(4 - \mathcal{L}). \quad (9)$$

A measure of entanglement between two coupled modes resembling (8) was introduced in [18] (where it was named “group correlation coefficient”):

$$\mathcal{K}^2 = 1 - \frac{\det \mathcal{Q}}{\det \mathcal{Q}_{11} \det \mathcal{Q}_{22}} = \tilde{\mathcal{L}} \left(2 - \tilde{\mathcal{L}} \right). \quad (10)$$

In principle, the measures (8) and (10) can be used for arbitrary (not only Gaussian) states, although sometimes they can give zero value even for truly entangled states (if the matrix of the second-order variances is factorized but intermode correlations exist for higher-order moments). Also, instead of (7) one could use the following extension of formula (10) to arbitrary states:

$$\tilde{\mathcal{K}}^2 = 1 - \left(\frac{\mu_1\mu_2}{\mu} \right)^2. \quad (11)$$

2.2. Distance Entanglement Measure

Another possibility to characterize entanglement is to use the Hilbert–Schmidt distance between given states and different “disentangled” states. This was considered, e.g., in [7, 12, 13] (an analogous approach was developed in [19] to quantify the “degree of nonclassicality” of quantum states). In [13] the entanglement measure was defined as $\text{Tr}(\hat{\rho} - \hat{\rho}_1 \otimes \hat{\rho}_2)^2$. However, we prefer to normalize it by $\text{Tr} \hat{\rho}^2$

so that the entanglement measure would not go to zero for highly mixed states. Thus we shall consider the following quantity:

$$\mathcal{Z} = \frac{\text{Tr}(\hat{\rho} - \hat{\rho}_1 \otimes \hat{\rho}_2)^2}{\text{Tr}\hat{\rho}^2} \equiv 1 + \frac{\mu_1\mu_2}{\mu} - \frac{2}{\mu} \text{Tr}(\hat{\rho} \cdot [\hat{\rho}_1 \otimes \hat{\rho}_2]). \quad (12)$$

For any states $\hat{\rho}$ and \hat{R} , one has (the normalization factor corresponds here to the two-mode case)

$$\text{Tr}(\hat{\rho}\hat{R}) = \int W_\rho(\mathbf{q})W_R(\mathbf{q}) \frac{d\mathbf{q}}{(2\pi)^2}. \quad (13)$$

For Gaussian states (3), the integrals can be calculated with the aid of the known formula

$$\int \exp(-\mathbf{q}A\mathbf{q} + \mathbf{b}\mathbf{q}) d\mathbf{q} = [\det(A/\pi)]^{-1/2} \exp\left(\frac{1}{4}\mathbf{b}A^{-1}\mathbf{b}\right). \quad (14)$$

The inverse matrix \mathcal{Q}^{-1} can be represented in the block form with the aid of the Frobenius formula [17]

$$\left\| \begin{array}{cc} \mathcal{Q}_{11} & \mathcal{Q}_{12} \\ \mathcal{Q}_{21} & \mathcal{Q}_{22} \end{array} \right\|^{-1} = \left\| \begin{array}{cc} \mathcal{Q}_{11}^{-1} + \mathcal{Q}_{11}^{-1}\mathcal{Q}_{12}\mathcal{Q}_*^{-1}\mathcal{Q}_{21}\mathcal{Q}_{11}^{-1} & -\mathcal{Q}_{11}^{-1}\mathcal{Q}_{12}\mathcal{Q}_*^{-1} \\ -\mathcal{Q}_*^{-1}\mathcal{Q}_{21}\mathcal{Q}_{11}^{-1} & \mathcal{Q}_*^{-1} \end{array} \right\|, \quad (15)$$

$$\mathcal{Q}_* = \mathcal{Q}_{22} - \mathcal{Q}_{21}\mathcal{Q}_{11}^{-1}\mathcal{Q}_{12}.$$

Taking into account Eqs. (3), (4), (14), and (15), one can verify that the Wigner function of the factorized state $\hat{\rho}_1 \otimes \hat{\rho}_2$ is given by formula (3) with the block-diagonal matrix

$$\mathcal{Q}_d = \left\| \begin{array}{cc} \mathcal{Q}_{11} & 0 \\ 0 & \mathcal{Q}_{22} \end{array} \right\|,$$

where matrices \mathcal{Q}_{11} and \mathcal{Q}_{22} are the same as in (4) (this is obvious from the physical point of view). Thus we arrive at the following expression for the \mathcal{Z} -measure (it is equivalent, except for the normalizing factor μ^{-1} , to that given in [13] but is written in a more simple explicit form):

$$\mathcal{Z} = 1 + \sqrt{\frac{\det \mathcal{Q}}{\det \mathcal{Q}_{11} \det \mathcal{Q}_{22}}} - 2\sqrt{\frac{\det(2\mathcal{Q})}{\det \mathcal{Q}_z}}, \quad \mathcal{Q}_z = \mathcal{Q} + \mathcal{Q}_d = \left\| \begin{array}{cc} 2\mathcal{Q}_{11} & \mathcal{Q}_{12} \\ \mathcal{Q}_{21} & 2\mathcal{Q}_{22} \end{array} \right\|. \quad (16)$$

2.3. Covariance Entanglement Measures

Other measures of entanglement have been introduced recently in [14, 15]. They are expressed directly in terms of the cross-covariances of the quadrature components or the equivalent annihilation/creation operators as follows:

$$\begin{aligned} \mathcal{Y} &= \left[\frac{\text{Tr}(\mathcal{Q}_{12}\mathcal{Q}_{21})}{\text{Tr}\mathcal{Q}_{11}\text{Tr}\mathcal{Q}_{22}} \right]^{1/2} \\ &= \left[\frac{|\overline{a_1 a_2^\dagger}|^2 + |\overline{a_1 a_2}|^2}{2 \left(\overline{a_1^\dagger a_1} + 1/2 \right) \left(\overline{a_2^\dagger a_2} + 1/2 \right)} \right]^{1/2} \\ &= \left[\frac{(\overline{x_1 x_2})^2 + (\overline{p_1 p_2})^2 + (\overline{x_1 p_2})^2 + (\overline{p_1 x_2})^2}{4\mathcal{E}_1\mathcal{E}_2} \right]^{1/2}, \end{aligned} \quad (17)$$

$$\begin{aligned}
 \tilde{\mathcal{Y}} &= \frac{2\sqrt{\text{Tr}(\mathcal{Q}_{12}\mathcal{Q}_{21})}}{\text{Tr}\mathcal{Q}} \\
 &= \frac{\sqrt{2\left(|\overline{a_1 a_2^\dagger}|^2 + |\overline{a_1 a_2}|^2\right)}}{\overline{a_1^\dagger a_1} + \overline{a_2^\dagger a_2} + 1} \\
 &= \frac{\sqrt{(\overline{x_1 x_2})^2 + (\overline{p_1 p_2})^2 + (\overline{x_1 p_2})^2 + (\overline{p_1 x_2})^2}}{\mathcal{E}_1 + \mathcal{E}_2},
 \end{aligned} \tag{18}$$

where (we use properly normalized dimensionless quadrature variables)

$$\hat{a}_k = \frac{\hat{x}_k + i\hat{p}_k}{\sqrt{2}}, \quad \mathcal{E}_k = \overline{a_k^\dagger a_k} + \frac{1}{2} \equiv \frac{1}{2} (\overline{x_k x_k} + \overline{p_k p_k}), \quad k = 1, 2. \tag{19}$$

Since the coefficients (17) and (18) are expressed in terms of traces of products of the off-diagonal blocks of the total covariance matrix \mathcal{Q} , they are obviously invariant with respect to the rotations in the phase plane of each subsystem. (Another invariant quantity, namely the determinant of the off-diagonal blocks $\det \mathcal{Q}_{12}$, plays an important role for the problem of separability of continuous variable systems [20].) It can be shown that $0 \leq \tilde{\mathcal{Y}} \leq \mathcal{Y} < 1$.

We would like to emphasize that the coefficients \mathcal{Y} and $\tilde{\mathcal{Y}}$ are defined for any (not only Gaussian) quantum state. They are significantly simpler than other entanglement measures from the viewpoint of calculations (calculating traces of matrices is much easier than calculating determinants, not to mention calculating eigenvalues of density operators or matrices, which are necessary to obtain the entropic measures). A disadvantage of the coefficients \mathcal{Y} and $\tilde{\mathcal{Y}}$ is that, in some cases, they are equal to zero for entangled state and the second-order moments of quadrature components are equal to zero. However, this does not take place for Gaussian and many other important quantum states.

2.4. Entropic Measures for Gaussian States

In order to demonstrate how simple are the expressions given in the previous sections compared with the “standard” entropic measure (1), we present here the formula for entropy of a generic Gaussian state. It is also determined by the covariance matrix but in a more complicated way than the coefficients considered above. For an arbitrary N -mode Gaussian state, the entropy was found in different but equivalent forms in [21, 22] and recently in [23]. The most simple expression is [24]

$$S_N = \sum_{j=1}^N \left[(\kappa_j + 1/2) \ln(\kappa_j + 1/2) - (\kappa_j - 1/2) \ln(\kappa_j - 1/2) \right], \tag{20}$$

where $\kappa_j \geq 1/2$ ($j = 1, \dots, N$) are N positive eigenvalues of matrix \mathcal{X} , which is the “ratio” of the symmetric covariance matrix \mathcal{Q} and antisymmetric commutator matrix:

$$\mathcal{X} \equiv \mathcal{Q} \Omega^{-1}, \quad \mathcal{Q}_{jk} = \frac{1}{2} \langle \hat{q}_j \hat{q}_k + \hat{q}_k \hat{q}_j \rangle, \quad \Omega_{jk} = \langle \hat{q}_j \hat{q}_k - \hat{q}_k \hat{q}_j \rangle. \tag{21}$$

One can easily verify that if κ is an eigenvalue of \mathcal{X} , then $-\kappa$ is the other eigenvalue. Also, it can be shown that all eigenvalues of \mathcal{X} are real. It is worth emphasizing that formula (20) is valid for arbitrary

sets of operators with c -number commutators (canonical coordinates and momenta, “annihilation” and “creation” operators, kinetic momenta and relative coordinates for particles moving in homogeneous magnetic fields, etc.).

In the one-mode case, the eigenvalues of matrix \mathcal{X} are equal to $\pm\kappa$ (and $\mathcal{X}^2 = \kappa^2 E_2$), where

$$\kappa = \hbar^{-1} \sqrt{\Delta}, \quad \Delta \equiv \overline{x x} \overline{p p} - (\widetilde{x p})^2 \geq \frac{\hbar^2}{4} = \det \mathcal{Q}. \quad (22)$$

(The last inequality is the Schrödinger–Robertson uncertainty relation [25–27].) In this case, different expressions equivalent to formula (20) were found in [21, 28, 29].

Calculating the characteristic polynomial of the 4×4 matrix \mathcal{X} in the two-mode case, one arrives at the biquadratic equation (for $\hbar = 1$) [22]

$$\kappa^4 - \mathcal{D}_2 \kappa^2 + \mathcal{D}_0 = 0, \quad (23)$$

where coefficients \mathcal{D}_2 and \mathcal{D}_0 are nothing but quantum universal invariants, i.e., functions which are invariant with respect to arbitrary linear canonical (preserving commutation relations) transformations [30]:

$$\mathcal{D}_2 = \Delta_1 + \Delta_2 + 2(\overline{x_1 x_2} \overline{p_1 p_2} - \overline{p_1 x_2} \overline{p_2 x_1}), \quad (24)$$

$$\begin{aligned} \mathcal{D}_0^{(2)} = \det \mathcal{Q} = & \left(\overline{p_1^2} \overline{p_2^2} - \overline{p_1 p_2}^2 \right) \left(\overline{x_1^2} \overline{x_2^2} - \overline{x_1 x_2}^2 \right) + (\overline{x_1 p_1} \overline{x_2 p_2} - \overline{x_1 p_2} \overline{x_2 p_1})^2 \\ & - \overline{x_2^2} \overline{p_1^2} (\overline{x_1 p_2})^2 - \overline{x_1^2} \overline{p_2^2} (\overline{x_2 p_1})^2 - \overline{x_2^2} \overline{p_2^2} (\overline{x_1 p_1})^2 - \overline{x_1^2} \overline{p_1^2} (\overline{x_2 p_2})^2 \\ & + 2 \overline{x_1 x_2} \left[\overline{p_1^2} \overline{x_1 p_2} \overline{x_2 p_2} + \overline{p_2^2} \overline{x_2 p_1} \overline{x_1 p_1} \right] + 2 \overline{p_1 p_2} \left[\overline{x_2^2} \overline{x_1 p_2} \overline{x_1 p_1} + \overline{x_1^2} \overline{x_2 p_1} \overline{x_2 p_2} \right] \\ & - 2 \overline{x_1 x_2} \overline{p_1 p_2} (\overline{x_1 p_1} \overline{x_2 p_2} + \overline{x_1 p_2} \overline{x_2 p_1}). \end{aligned} \quad (25)$$

The symbol Δ_k , obviously, means the combination defined by (22) and related to the k th mode.

Positive solutions of Eq. (23) read

$$\kappa_{1,2} = \frac{1}{2} \left[\sqrt{\mathcal{D}_2 + 2\sqrt{\mathcal{D}_0}} \pm \sqrt{\mathcal{D}_2 - 2\sqrt{\mathcal{D}_0}} \right]. \quad (26)$$

The reality of $\kappa_{1,2}$ is ensured by the inequalities

$$\mathcal{D}_2 \geq 2\sqrt{\mathcal{D}_0} \geq \frac{\hbar^2}{2}, \quad (27)$$

which can be considered as generalized uncertainty relations for two-mode systems (for systematic studies of such generalizations see, e.g., [27, 31]).

Formulas (20), (22), and (26) permit one to express the entropic index of correlation (1) analytically in terms of the covariances of quadrature components for arbitrary Gaussian states. However, the corresponding expression is very cumbersome, and it is much more complicated than any other entanglement measure discussed in the previous sections. In the following sections, we compare the behavior of different entanglement measures for various concrete physical models.

3. Three-Dimensional Cavity with Vibrating Wall and Two Resonantly Coupled Modes

Classical and quantum phenomena in cavities with moving boundaries have attracted the attention of many researchers for a long time (see review [32]). This topic became especially popular in the last decade, being known now under the names nonstationary Casimir effect [33], dynamical Casimir effect [34], or mirror (motion) induced radiation [35, 36]. One of several theoretical results obtained in the last years was the prediction of the exponential growth of the field energy under resonance conditions where the wall vibrates at a frequency that is a multiple of the unperturbed field eigenfrequency [16, 36, 37].

A unified description of the field inside an ideal cavity with moving boundaries can be achieved within the frameworks of the Hamiltonian approach proposed by Law [37] and developed in [38] (for other references, see [32]; for the most recent publications, see [39–41]). Consider a scalar massless field $\Phi(\mathbf{r}, t)$ satisfying the wave equation

$$\Phi_{tt} = \nabla^2 \Phi$$

inside the cavity and the Dirichlet boundary condition

$$\Phi = 0$$

on the boundary (we put $c = \hbar = 1$). We assume that we know the complete orthonormalized set of eigenfunctions (and eigenfrequencies) of the Laplace equation

$$\nabla^2 f_\alpha(\mathbf{r}) + \omega_\alpha^2 f_\alpha(\mathbf{r}) = 0$$

in the case of a stationary cavity. Now suppose that a part of the boundary is a plane surface moving according to a prescribed law of motion $L(t)$ (for the most recent study of the case where $L(t)$ is a dynamical variable due to the back reaction of the field, see [42]). Expanding the field $\Phi(\mathbf{r}, t)$ over “instantaneous” eigenfunctions $f_\alpha(\mathbf{r}; L(t))$

$$\Phi(\mathbf{r}, t) = \sum_{\alpha} q_{\alpha}(t) f_{\alpha}(\mathbf{r}; L(t)), \quad (28)$$

we satisfy automatically the boundary conditions. Then the field dynamics is described completely by the dynamics of the generalized coordinates $q_{\alpha}(t)$, which, in turn, can be derived from the time-dependent Hamiltonian [38]

$$H(t) = \frac{1}{2} \sum_{\alpha} [p_{\alpha}^2 + \omega_{\alpha}^2(L(t)) q_{\alpha}^2] + \frac{\dot{L}(t)}{L(t)} \sum_{\alpha \neq \beta} p_{\alpha} m_{\alpha\beta} q_{\beta} \quad (29)$$

with antisymmetric time-independent coefficients

$$m_{\alpha\beta} = -m_{\beta\alpha} = L \int dV \frac{\partial f_{\alpha}(\mathbf{r}; L)}{\partial L} f_{\beta}(\mathbf{r}; L). \quad (30)$$

For example, in the case of a rectangular three-dimensional cavity with dimensions L_x , L_y , and L_z , the eigenmodes are well-known products of sine functions like $\sin(\pi k_x x / L_x)$ (or sine and cosine functions in

the case of electromagnetic field) labeled by three natural numbers k_x , k_y , and k_z , whereas unperturbed eigenfrequencies are given by the formula

$$\omega_{k_x, k_y, k_z} = \pi \sqrt{\left(\frac{k_x}{L_x}\right)^2 + \left(\frac{k_y}{L_y}\right)^2 + \left(\frac{k_z}{L_z}\right)^2}. \quad (31)$$

If one surface of the parallelepiped perpendicular to the x axis moves in the x direction (so that the L_x dimension of the cavity is a function of time), then [43]

$$m_{\mathbf{kj}} = (-1)^{k_x + j_x} \frac{2k_x j_x}{j_x^2 - k_x^2} \delta_{k_y j_y} \delta_{k_z j_z}. \quad (32)$$

(In the case of an electromagnetic field, one should take into account polarizations of the modes, i.e., that f_α and f_β in Eq. (30) are vector functions, whose directions are perpendicular, respectively, to the vectors (k_x, k_y, k_z) and (j_x, j_y, j_z) . But one can always choose two modes with coinciding polarizations directed along the perpendicular to the plane formed by these two vectors. Then all formulas are the same as in the scalar case.)

We are interested in the case where one of the cavity's walls performs small oscillations with frequency Ω close to twice the frequency of some unperturbed mode

$$\omega_1^{(0)} \equiv 1$$

(i.e., we normalize all frequencies by $\omega_1^{(0)}$), so that the time-dependent frequency $\omega_1(t)$ reads

$$\omega_1(t) = 1 + 2\epsilon \cos(2\bar{\omega}t), \quad \bar{\omega} = 1 + \delta, \quad (33)$$

where we assume that

$$|\delta| \ll 1 \quad \text{and} \quad |\epsilon| \ll 1.$$

Also we suppose that the unperturbed field frequency spectrum includes the frequency

$$\omega_3^{(0)} = 3 + \Delta \quad \text{with} \quad |\Delta| \ll 1$$

but it does not contain frequencies close to $5\omega_1^{(0)}$. A possibility of such a situation was pointed out in [43]. An example is a cubic cavity with the pair of modes $\{111\}$ and $\{511\}$. Another example is the pair of modes $\{110\}$ and $\{510\}$ in the rectangular cavity with $L_x = \sqrt{2}L_y$ (in this case, the common direction of polarization is along the z axis). Then we have two resonantly interacting modes, and it is sufficient to consider only the part of the total Hamiltonian (29) related to these modes [44] (hereafter, we use the symbols x_k, p_j instead of q_k, p_j for the quadrature components of the field, whereas the x without indices means the usual space coordinate inside the cavity):

$$\begin{aligned} H_{13} = & \frac{1}{2} (p_1^2 + p_3^2) + \frac{1}{2} [1 + 4\epsilon \cos(2\bar{\omega}t)] x_1^2 + \frac{1}{2} [9 + 6\Delta + \tilde{\epsilon} \cos(2\bar{\omega}t)] x_3^2 \\ & + 3\mu\epsilon \sin(2\bar{\omega}t) (p_1 x_3 - p_3 x_1). \end{aligned} \quad (34)$$

The constant parameter μ is proportional to the coefficient m_{12} in (29).

For the rectangular cavity, $\mu = j_x/(12k_x)$ if the modes $\{k_x, m, n\}$ and $\{j_x, m, n\}$ are in resonance. Writing (34) we have neglected second-order terms with respect to ϵ and Δ . Parameter $\tilde{\epsilon}$ has the same order of magnitude as ϵ but it does not affect the solution in the zeroth-order approximation [44].

Hamiltonian (34) results in the following differential equations for the generalized coordinates x_1 and x_3 (we neglect corrections of the second order):

$$\ddot{x}_1 = -\left[1 + 4\epsilon \cos(2\bar{\omega}t)\right]x_1 + 24\mu\epsilon \left[\cos(2\bar{\omega}t)x_3 + \sin(2\bar{\omega}t)\dot{x}_3\right], \tag{35}$$

$$\ddot{x}_3 = -\left[9 + 6\Delta + \tilde{\epsilon} \cos(2\bar{\omega}t)\right]x_3 - 24\mu\epsilon \left[\cos(2\bar{\omega}t)x_1 + \sin(2\bar{\omega}t)\dot{x}_1\right]. \tag{36}$$

These equations have been solved, in view of the method of slowly varying amplitudes, in [44]. We consider here two special cases.

3.1. Exact (Symmetric) Resonance

In the case of exact resonance, $\delta = \Delta = 0$, the solutions of Eqs. (35) and (36) read

$$\begin{aligned} x_1(t) = & x_1(0) \left[C_1^- \cos(\rho\tau) + S_1^- \frac{\sin(\rho\tau)}{\rho} \right] - p_1(0) \left[S_1^- \cos(\rho\tau) + C_1^- \frac{\sin(\rho\tau)}{\rho} \right] \\ & + 8\mu \frac{\sin(\rho\tau)}{\rho} \left[3S_1^- x_3(0) + C_1^- p_3(0) \right], \end{aligned} \tag{37}$$

$$\begin{aligned} x_3(t) = & x_3(0) \left[C_3^+ \cos(\rho\tau) - S_3^+ \frac{\sin(\rho\tau)}{\rho} \right] + \frac{1}{3}p_3(0) \left[S_3^+ \cos(\rho\tau) - C_3^+ \frac{\sin(\rho\tau)}{\rho} \right] \\ & - 8\mu \frac{\sin(\rho\tau)}{\rho} \left[S_3^+ x_1(0) - C_3^+ p_1(0) \right], \end{aligned} \tag{38}$$

$$\begin{aligned} p_1(t) = & -x_1(0) \left[S_1^+ \cos(\rho\tau) + C_1^+ \frac{\sin(\rho\tau)}{\rho} \right] + p_1(0) \left[C_1^+ \cos(\rho\tau) + S_1^+ \frac{\sin(\rho\tau)}{\rho} \right] \\ & - 8\mu \frac{\sin(\rho\tau)}{\rho} \left[3C_1^+ x_3(0) + S_1^+ p_3(0) \right], \end{aligned} \tag{39}$$

$$\begin{aligned} p_3(t) = & 3x_3(0) \left[S_3^- \cos(\rho\tau) - C_3^- \frac{\sin(\rho\tau)}{\rho} \right] + p_3(0) \left[C_3^- \cos(\rho\tau) - S_3^- \frac{\sin(\rho\tau)}{\rho} \right] \\ & - 24\mu \frac{\sin(\rho\tau)}{\rho} \left[C_3^- x_1(0) - S_3^- p_1(0) \right], \end{aligned} \tag{40}$$

where

$$C_k^\pm(\tau; t) = \cosh \tau \cos(k\bar{\omega}t) \pm \sinh \tau \sin(k\bar{\omega}t), \quad S_k^\pm(\tau; t) = \sinh \tau \cos(k\bar{\omega}t) \pm \cosh \tau \sin(k\bar{\omega}t), \tag{41}$$

$$\tau \equiv \frac{1}{2} \epsilon t, \quad \rho = \sqrt{2\nu - 1}, \quad \nu \equiv 96 \mu^2. \tag{42}$$

The arguments t (“fast time”) and τ (“slow time”) of the functions $C_k^\pm(\tau; t)$ and $S_k^\pm(\tau; t)$ can be considered as independent variables. Then the following relations hold:

$$\frac{\partial C_k^\pm}{\partial t} = \pm k S_k^\mp, \quad \frac{\partial S_k^\pm}{\partial t} = \pm k C_k^\mp. \tag{43}$$

For the modes {111} and {511} of the cubic cavity or {110} and {510} of the rectangular cavity with $L_x = \sqrt{2}L_y$, one has $\nu = 50/3$. Due to this explicit example, we assume that the parameter ν is large, $\nu \gg 1$.

Symbols x_k and p_k in Eqs. (37)–(40) can be considered both as classical variables and quantum operators in the Heisenberg picture, due to the linearity of the problem [or due to the quadratic nature of Hamiltonian (29)]. In view of Eqs. (37)–(40), one can calculate mean values of squares and products of canonical variables (operators) at any time moment provided such mean values were known at the initial time moment $t = 0$. We confine ourselves to the case where the field modes were initially in thermal states with the mean photon numbers $(\theta_1 - 1)/2$ and $(\theta_3 - 1)/2$, where $\theta_k = \coth(k\beta_k/2)$, with β_k being the inverse absolute temperature in dimensionless units. In the natural case of equal initial temperatures of the modes, the following relations hold:

$$\theta_{31} \equiv \frac{\theta_3}{\theta_1} = \theta_{13}^{-1} = \frac{\theta_1^2 + 3}{3\theta_1^2 + 1}, \quad 1 \geq \theta_{31} \geq \frac{1}{3}. \tag{44}$$

The normalized mean energies in each mode

$$\mathcal{E}_k = \frac{\langle p_k^2 + \omega_k^2 x_k^2 \rangle}{2\omega_k}$$

[namely these quantities are used in the definitions of the covariance entanglement coefficients (17) and (18)] depend on time as follows [44]:

$$\mathcal{E}_1 = \frac{\theta_1}{2} \left\{ \cosh(2\tau) \left[\frac{\sin^2(\rho\tau)}{\rho^2} (1 + 2\nu\theta_{31}) + \cos^2(\rho\tau) \right] + \sinh(2\tau) \frac{\sin(2\rho\tau)}{\rho} \right\}, \tag{45}$$

$$\mathcal{E}_3 = \frac{\theta_3}{2} \left\{ \cosh(2\tau) \left[\frac{\sin^2(\rho\tau)}{\rho^2} (1 + 2\nu\theta_{13}) + \cos^2(\rho\tau) \right] - \sinh(2\tau) \frac{\sin(2\rho\tau)}{\rho} \right\}. \tag{46}$$

Calculating the covariance entanglement coefficient, one should use, instead of variables x_k and p_k , the normalized variables

$$\tilde{x}_k = \sqrt{\omega_k} x_k \quad \text{and} \quad \tilde{p}_k = \frac{p_k}{\sqrt{\omega_k}}$$

(in our case $\omega_k \equiv k$); see Eq. (19). After some algebra, we obtain the following expressions:

$$\mathcal{Y} = \sqrt{\frac{\mathcal{F}}{4\mathcal{E}_1\mathcal{E}_3}}, \quad \tilde{\mathcal{Y}} = \frac{\sqrt{\mathcal{F}}}{\mathcal{E}_1 + \mathcal{E}_3}, \tag{47}$$

$$\begin{aligned} \mathcal{F} = & \frac{\nu}{2\nu - 1} \sin^2(\rho\tau) \left\{ \cosh(4\tau) \left[\cos^2(\rho\tau) (\theta_1 - \theta_3)^2 + \frac{\sin^2(\rho\tau)}{\rho^2} (\theta_1 + \theta_3)^2 \right] \right. \\ & \left. + \frac{\sin(2\rho\tau)}{\rho} \sinh(4\tau) (\theta_1^2 - \theta_3^2) \right\}. \end{aligned} \tag{48}$$

The determinants of the covariance matrices for each mode have been calculated in [44]. For the first mode,

$$\det \mathcal{Q}_{11} = \frac{1}{4} \theta_1^2 g_1^2, \quad g_1^2 = \cos^4(\rho\tau) + \sin^2(2\rho\tau) \frac{2\nu\theta_{31} - 1}{2(2\nu - 1)} + \sin^4(\rho\tau) \left(\frac{2\nu\theta_{31} + 1}{2\nu - 1} \right)^2. \tag{49}$$

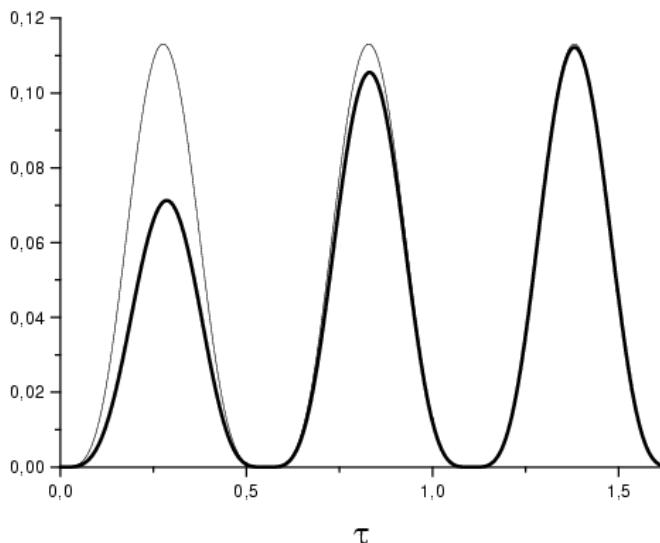


Fig. 1. Covariance entanglement coefficient squared \mathcal{Y}^2 (thick line) and purity entanglement coefficient $\tilde{\mathcal{L}}$ (thin line) versus “slow time” τ for two interacting modes $\{1, 1, 1\}$ and $\{5, 1, 1\}$ in a 3D cubic cavity ($\nu = 50/3$) under the strict (“symmetric”) resonance condition for the initial vacuum state.

For the other excited mode, one should interchange indices 1 and 3 in (49). Since, in the case under discussion, the evolution of the total system is unitary, the total determinant does not depend on time

$$\det Q = \frac{\theta_1^2 \theta_3^2}{16}.$$

Therefore, the purity entanglement coefficient (8) has the form

$$\tilde{\mathcal{L}} = 1 - (g_1 g_3)^{-1}. \tag{50}$$

Equations (20) and (22) lead to the following explicit formula for the entropy entanglement measure I_c (1):

$$I_c = \frac{1}{2} \sum_{i=1,3} \left[(\theta_i g_i + 1) \ln (\theta_i g_i + 1) - (\theta_i g_i - 1) \ln (\theta_i g_i - 1) - (\theta_i + 1) \ln (\theta_i + 1) + (\theta_i - 1) \ln (\theta_i - 1) \right]. \tag{51}$$

We see that despite the exponential (although nonmonotonous in the high-temperature case $\theta_k \gg 1$ [44]) growth in energy of each mode, all entanglement coefficients exhibit strong (quasi)periodic oscillations as functions of the “slow time” τ , going to zero when $\rho\tau = n\pi$.

In the simplest case of the initial vacuum states of each mode ($\theta_1 = \theta_3 = 1$), one has

$$\mathcal{F} = \frac{4\nu}{(2\nu - 1)^2} \sin^4(\rho\tau) \cosh(4\tau), \tag{52}$$

$$g_1^2 = g_3^2 = g_0^2 \equiv 1 + \frac{8\nu}{(2\nu - 1)^2} \sin^4(\rho\tau), \tag{53}$$

$$\tilde{\mathcal{L}} = \frac{8\nu \sin^4(\rho\tau)}{(2\nu - 1)^2 + 8\nu \sin^4(\rho\tau)} \approx \frac{2}{\nu} \sin^4(\rho\tau), \tag{54}$$

$$I_c = (g_0 + 1) \ln(g_0 + 1) - (g_0 - 1) \ln(g_0 - 1) - 2 \ln 2 \approx \frac{\sin^4(\rho\tau)}{\nu} \ln\left(\frac{2e\nu}{\sin^4(\rho\tau)}\right). \tag{55}$$

The approximate equalities in (54) and (55) hold for $\nu \gg 1$. Under this condition,

$$\mathcal{E}_1 \approx \mathcal{E}_3 \approx \frac{1}{2} \cosh(2\tau),$$

so that for $\tau > 1$ one obtains

$$\mathcal{Y} \approx \sqrt{\frac{2}{\nu}} \sin^2(\rho\tau) \approx \sqrt{\tilde{\mathcal{L}}}.$$

The evolution of functions $\tilde{\mathcal{L}}(\tau)$ and $\mathcal{Y}^2(\tau)$ for the initial vacuum state is shown in Fig. 1.

For high-temperature initial states ($\theta_{1,3} \gg 1$), the entanglement coefficients do not depend on the parameter ν (if $\nu \gg 1$) for almost all instants of time; more precisely, under the condition

$$|\cos(\rho\tau)| \gg \rho^{-1} \sim \nu^{-1/2},$$

one has

$$\tilde{\mathcal{L}} \approx \frac{\sin^2(2\rho\tau) (\theta_{31} + \theta_{13} - 2)}{4 + \sin^2(2\rho\tau) (\theta_{31} + \theta_{13} - 2)} \approx \mathcal{Y}^2, \tag{56}$$

$$I_c = \ln(g_1 g_3) \approx \ln\left[1 + \frac{1}{4} \sin^2(2\rho\tau) (\theta_{31} + \theta_{13} - 2)\right]. \tag{57}$$

(The last approximate equality in (56) holds for $\tau > 1$. The simple formula for I_c is obtained in the limit case $\theta_{1,3} \rightarrow \infty$; there are some corrections of the order of $\theta_{1,3}^{-1}$ for finite initial mean numbers of photons.) For the maximum possible value of the coefficient $\theta_{13} = 3$ (in the case of true initial thermal equilibrium), the maximum values of expressions (56) and (57) (which are achieved when $\sin^2(2\rho\tau) = 1$) are equal to

$$\tilde{\mathcal{L}}_{\max} = \frac{1}{4} \quad \text{and} \quad I_c^{(\max)} = \ln(4/3) \approx \frac{1}{3}.$$

Note that in the limit high-temperature case, the purity entanglement coefficient coincides identically with one of the possible forms of the ‘‘compact entropy’’ (another compact parameter $\tanh(I_c)$ was introduced in [14])

$$\mathcal{J}_c = 1 - \exp(-I_c). \tag{58}$$

Figure 2 shows the evolution of entropy entanglement measure $I_c(\tau)$ for the vacuum and high-temperature initial states. Note that one has $\theta_1 \approx 140$, if $L_0 = 1$ cm and $T = 300$ K. For this value of θ_1 , the plot of the compact entropy $\mathcal{J}_c(\tau)$ becomes indistinguishable from the plot of the purity entanglement coefficient $\tilde{\mathcal{L}}(\tau)$. The functions $\tilde{\mathcal{L}}(\tau)$ and $\mathcal{Y}^2(\tau)$ are compared in Fig. 3. We see that the two functions are very close in some intervals, although their maxima are different (because the value $\rho \approx 5.7$ is not very large for the chosen parameter $\nu = 50/3$).

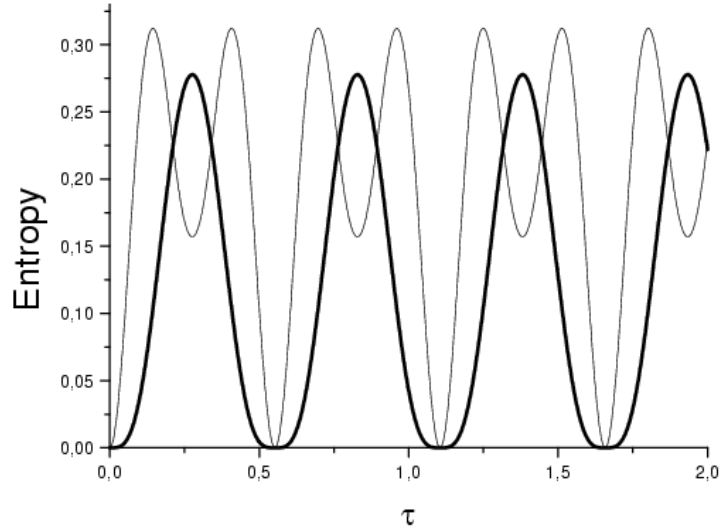


Fig. 2. Entropy entanglement measure I_c (51) versus “slow time” τ for two interacting modes $\{1, 1, 1\}$ and $\{5, 1, 1\}$ in a 3D cubic cavity ($\nu = 50/3$) under the strict (“symmetric”) resonance condition for the initial vacuum state at $\theta_1 = \theta_3 = 1$ (thick line) and for the high-temperature state at $\theta_1 = 3\theta_3$ (thin line).

In the high-temperature case, intermediate nonzero minima of the entanglement coefficients (besides exact zero minima at the time instant $\tau_n = n\pi/\rho$) are observed at the “slow time” moments when the modes approximately exchange their purities [44]. The positions of these additional minima for $\tilde{\mathcal{L}}$ and I_c are determined by the condition $\cos(\rho\tau) = 0$, so that

$$\tilde{\mathcal{L}}_{\min} = \frac{2\nu(\theta_{31} + \theta_{13} + 2)}{4\nu^2 + 1 + 2\nu(\theta_{31} + \theta_{13})}, \quad I_c^{(\min)} = \ln \left[1 + \frac{2\nu(\theta_{31} + \theta_{13} + 2)}{(2\nu - 1)^2} \right]. \quad (59)$$

For $\nu \gg 1$, one has

$$\tilde{\mathcal{L}}_{\min} \approx I_c^{(\min)} \approx \frac{\theta_{31} + \theta_{13} + 2}{2\nu}. \quad (60)$$

On the other hand, the intermediate minima of \mathcal{Y} are much smaller. Indeed, the minimum of the expression inside the curly brackets in Eq. (48) is achieved for (while neglecting corrections of the order of ρ^{-3})

$$\tan(2\rho\tau) = \frac{2}{\rho} \tanh(4\tau) \frac{\theta_1 + \theta_3}{\theta_1 - \theta_3}.$$

At this time moment, one obtains

$$\mathcal{F} \approx \frac{(\theta_1 + \theta_3)^2}{4\nu \cosh(4\tau)}, \quad 4\mathcal{E}_1\mathcal{E}_3 \approx \theta_1\theta_3 \cosh^2(2\tau),$$

so that for $\tau > 1$,

$$\mathcal{Y} \approx e^{-4\tau} \sqrt{\frac{2}{\nu}(\theta_{31} + \theta_{13} + 2)} \equiv \mathcal{Y}_* \approx 2e^{-4\tau} \sqrt{\tilde{\mathcal{L}}_{\min}},$$

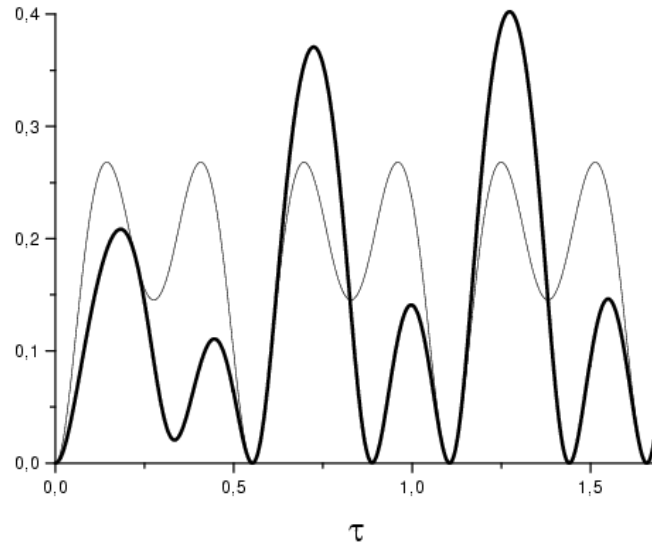


Fig. 3. Functions $\tilde{\mathcal{L}}(\tau)$ (thin line) and $\mathcal{Y}^2(\tau)$ (thick line) for two interacting modes $\{1, 1, 1\}$ and $\{5, 1, 1\}$ in a 3D cubic cavity ($\nu = 50/3$) under the strict (“symmetric”) resonance condition for the high-temperature initial state at $\theta_1 = 140$.

and it is clear that the intermediate minimum of \mathcal{Y} does not exceed the value \mathcal{Y}_* .

Therefore, we arrive at a rather paradoxical situation, especially for realistic values of parameters ν and $\theta_{1,3}$. According to Fig. 3, the intermediate minimum value of the $\tilde{\mathcal{L}}$ coefficient in the high-temperature case is only half the maximum value. Moreover, this high-temperature intermediate minimum value is bigger than the maximum value in the vacuum-state case (see Fig. 1). Thus, the $\tilde{\mathcal{L}}$ coefficient tells us that for $\cos(\rho\tau) = 0$ the two modes are “more entangled” in the high-temperature case than in the case of initial vacuum state (or at least have the same order of entanglement, according to the I_c coefficient in Fig. 2), whereas the covariance entanglement coefficient \mathcal{Y} shows that two modes become practically disentangled at this instant of time.

The resolution of this “paradox” is as follows. According to Eqs. (17), (47), and (48), the function \mathcal{F} arrives at the upper limit for squares of any elements of the “off-diagonal” block \mathcal{Q}_{12} of the covariance matrix \mathcal{Q} (4), whereas functions \mathcal{E}_k give the bounds for the elements of “diagonal” blocks \mathcal{Q}_{kk} . This happens because \mathcal{F} and \mathcal{E}_k are based on traces of the covariance submatrices. Therefore, if $\mathcal{Y} \rightarrow 0$, this means that all elements of matrix \mathcal{Q}_{12} responsible for the intermode correlations (at least for the Gaussian states considered in this section) become negligible in comparison with the variances $\overline{x_k x_k}$ and $\overline{p_k p_k}$ of the quadrature components. From the physical point of view, it is equivalent to the disappearance of correlations between the two subsystems, i.e., their disentanglement.

On the other hand, the coefficients $\tilde{\mathcal{L}}$ and I_c are based on determinants of the covariance submatrices. But it is well known that the determinant of a matrix can be quite small even if all elements of the matrix are big, and this is the reason for the qualitative difference in the behavior of the “covariance” and “entropic” entanglement coefficients. This is clearly seen from the last expression in Eq. (8), which

shows that the value of the purity entanglement coefficient $\tilde{\mathcal{L}}$ depends on the matrix

$$R = Q_{12} Q_{22}^{-1} Q_{21} Q_{11}^{-1}.$$

In view of the easily verified formula

$$\det(E + \alpha) \approx \text{Tr } \alpha,$$

which holds provided all elements of matrix α are small with respect to unity, we can simplify formula (8) in the case of small entanglement as follows:

$$\tilde{\mathcal{L}} \approx \frac{1}{2} \text{Tr} (Q_{12} Q_{22}^{-1} Q_{21} Q_{11}^{-1}). \quad (61)$$

But each matrix Q_{kk}^{-1} ($k = 1, 3$) contains the denominator $\det Q_{kk}$, which can be much less than any element of matrix Q_{kk} . If this happens, then the inequality

$$\text{Tr} (Q_{12} Q_{22}^{-1} Q_{21} Q_{11}^{-1}) \gg \frac{\text{Tr} (Q_{12} Q_{21})}{\text{Tr} Q_{11} \text{Tr} Q_{22}}$$

becomes quite possible. Just such a situation takes place in the example considered. Although diagonal elements $\overline{x_k x_k}$ and $\overline{p_k p_k}$ of matrices Q_{kk} grow exponentially with time, these matrices have also exponentially growing off-diagonal covariance elements $\widetilde{x_k p_k}$ (this means that each mode occurs in a highly-correlated quantum state [26] with the quadrature correlation coefficient

$$r \equiv \frac{\widetilde{x_k p_k}}{(\overline{x_k x_k} \overline{p_k p_k})^{1/2}}$$

approaching the unit value), so that $\det Q_{kk}$ does not grow unbounded with time, exhibiting only relatively small oscillations. For this reason, elements of matrices Q_{kk}^{-1} have the same order of magnitude $\sim \exp(2\tau)$ as elements of matrices Q_{kk} themselves. On the other hand, elements of matrix Q_{12} have the order of $\exp(-2\tau)$ at intermediate minima. Therefore, the exponential time dependences are canceled in the measures based on determinants, resulting in the inequalities

$$\mathcal{J}_c, \tilde{\mathcal{L}} \gg \mathcal{Y}_* \quad \text{for} \quad \cos(\rho\tau) \approx 0.$$

This example permits one to make a conjecture that the covariance entanglement coefficient \mathcal{Y} is not only simpler from the viewpoint of calculations but could be preferable from the physical point of view because it is more sensitive to entanglement than entropic and purity measures. Other arguments in favor of \mathcal{Y} can be found in [15].

3.2. Asymmetric Resonance

An interesting feature of the Hamiltonian (34) discovered in [44] is the possibility to compensate one detuning (e.g., δ) at the expense of another. In particular, an exponential growth of the energies of both modes can be obtained under the conditions of “asymmetric resonance”

$$\delta = \epsilon, \quad 3\delta - \Delta = \frac{\epsilon\nu}{2}. \quad (62)$$

In this case, the quadrature components depend on time as follows:

$$x_1(t) = x_1(0) \left[\left(1 - \frac{2}{\nu}\right) C_1^-(2R\tau; t) + \frac{2}{\nu} \cos \phi_1 \right] - p_1(0) \left[\left(1 - \frac{2}{\nu}\right) S_1^-(2R\tau; t) - \frac{2}{\nu} \sin \phi_1 \right] + \frac{x_3(0)}{4\mu} [C_1^-(2R\tau; t) - \cos \phi_1] - \frac{p_3(0)}{12\mu} [S_1^-(2R\tau; t) + \sin \phi_1], \quad (63)$$

$$x_3(t) = x_3(0) \left[\left(1 - \frac{2}{\nu}\right) \cos \phi_3 + \frac{2}{\nu} C_3^-(2R\tau; t) \right] + \frac{1}{3} p_3(0) \left[\left(1 - \frac{2}{\nu}\right) \sin \phi_3 - \frac{2}{\nu} S_3^-(2R\tau; t) \right] + \frac{x_1(0)}{12\mu} [C_3^-(2R\tau; t) - \cos \phi_3] - \frac{p_1(0)}{12\mu} [S_3^-(2R\tau; t) + \sin \phi_3], \quad (64)$$

$$p_1(t) = -x_1(0) \left[\left(1 - \frac{2}{\nu}\right) S_1^+(2R\tau; t) + \frac{2}{\nu} \sin \phi_1 \right] + p_1(0) \left[\left(1 - \frac{2}{\nu}\right) C_1^+(2R\tau; t) + \frac{2}{\nu} \cos \phi_1 \right] - \frac{x_3(0)}{4\mu} [S_1^+(2R\tau; t) - \sin \phi_1] + \frac{p_3(0)}{12\mu} [C_1^+(2R\tau; t) - \cos \phi_1], \quad (65)$$

$$p_3(t) = -3x_3(0) \left[\left(1 - \frac{2}{\nu}\right) \sin \phi_3 + \frac{2}{\nu} S_3^+(2R\tau; t) \right] + p_3(0) \left[\left(1 - \frac{2}{\nu}\right) \cos \phi_3 + \frac{2}{\nu} C_3^+(2R\tau; t) \right] - \frac{x_1(0)}{4\mu} [S_3^+(2R\tau; t) - \sin \phi_3] + \frac{p_1(0)}{4\mu} [C_3^+(2R\tau; t) - \cos \phi_3], \quad (66)$$

where

$$\phi_k(\tau; t) = k\bar{\omega}t - 2J\tau, \quad R = 1 - \frac{2}{\nu}, \quad J = \frac{\nu}{2} + 1,$$

and all terms of the order of $\mathcal{O}(\nu^{-2})$ are neglected (as well as corrections of the order of $\delta \sim \epsilon$ in the amplitude coefficients).

The (normalized) mean energies of each mode depend on time as follows [44]:

$$\mathcal{E}_1 = \frac{\theta_1}{2} \left[\left(1 - \frac{4}{\nu}\right) \cosh(4R\tau) + \frac{4}{\nu} \psi(\tau) \right] + \frac{\theta_3}{\nu} [\cosh(4R\tau) + 1 - 2\psi(\tau)], \quad (67)$$

$$\mathcal{E}_3 = \frac{\theta_3}{2} \left[1 - \frac{4}{\nu} + \frac{4}{\nu} \psi(\tau) \right] + \frac{\theta_1}{\nu} [\cosh(4R\tau) + 1 - 2\psi(\tau)], \quad (68)$$

where

$$\psi(\tau) \equiv \cosh(2R\tau) \cos(2J\tau).$$

The energy of the third mode is significantly less than the energy of the first mode, if $\nu \gg 1$. For this reason, this regime of excitation was named ‘‘asymmetrical’’

$$\text{for } \tau > 1, \quad \frac{\mathcal{E}_3}{\mathcal{E}_1} \approx \frac{6}{\nu}.$$

Note, however, that for a cubic cavity with $\nu = 50/3$ the energy of the third mode is only one-third than that of the first one. It is important, nonetheless, that the rates of increase in energies of each mode are almost twice those in the case of the strict resonance discussed in the previous section.

The covariance entanglement coefficients can be written again in form (47) but with $\mathcal{E}_{1,3}$ given by (67) and (68). The function \mathcal{F} in the asymmetric case reads (neglecting corrections of the order of ν^{-2} with respect to the main terms)

$$\begin{aligned} \mathcal{F} = & 2\nu^{-1} \left\{ \theta_1^2 \left(\cosh^2(4R\tau) + \sinh^2(2R\tau) - \cosh(6R\tau) \cos \phi_0 \right. \right. \\ & + 2\nu^{-1} \left[\cos \phi_0 \{ \cosh(2R\tau) + 3 \cosh(6R\tau) \} - 2 \cosh^2(2R\tau) \cos^2 \phi_0 - 2 \cosh(4R\tau) - 2 \sinh^2(4R\tau) \right] \\ & + \theta_3^2 \left(\cosh^2(2R\tau) - \cosh(2R\tau) \cos \phi_0 \right. \\ & + 2\nu^{-1} \left[\cos \phi_0 \{ \cosh(6R\tau) + 3 \cosh(2R\tau) \} - 2 \cosh^2(2R\tau) \cos^2 \phi_0 - 2 \cosh(4R\tau) \right] \\ & + 2\theta_1\theta_3 \left(\cosh(4R\tau) [\cosh(2R\tau) \cos \phi_0 - 1] \right. \\ & \left. \left. + 2\nu^{-1} \left[-2 \cos \phi_0 \{ \cosh(6R\tau) + \cosh(2R\tau) \} + 2 \cosh^2(2R\tau) \cos^2 \phi_0 + 4 \cosh^4(2R\tau) - 2 \right] \right) \right\}, \quad (69) \end{aligned}$$

where $\phi_0 = -2J\tau$.

If $\tau \rightarrow \infty$, then (for $\nu \gg 1$)

$$\mathcal{F} \approx \frac{\theta_1^2}{2\nu} e^{8R\tau}, \quad \mathcal{E}_1 \approx \frac{\theta_1}{4} e^{4R\tau}, \quad \mathcal{E}_3 \approx \frac{\theta_1}{2\nu} e^{4R\tau},$$

so that $\mathcal{Y} \rightarrow 1$, whereas $\tilde{\mathcal{Y}} \rightarrow \sqrt{8/\nu}$. Consequently, the coefficient \mathcal{Y} is preferable when the energies of subsystems are essentially different.

The purity and entropic entanglement coefficients are given by Eqs. (50) and (51) with

$$g_1^2(\tau) = 1 + \frac{8}{\nu} [(1 - \theta_{31}) \psi(\tau) - 1 + \theta_{31} \cosh^2(2R\tau)] \quad (70)$$

and g_3 obtained from (70) by means of the replacement $1 \leftrightarrow 3$. We see a significant difference from the strict resonance case — now functions $g_{1,3}(\tau)$ increase exponentially with time for $\tau \gg 1$. Asymptotically, each mode appears in a highly mixed quantum state, with

$$\det Q_{11} = \det Q_{33} = \theta_1\theta_3 \frac{\exp(4R\tau)}{2\nu}.$$

The purity entanglement coefficient (50) tends asymptotically to the unit value independently of the initial temperature (or coefficients θ_k):

$$\tilde{\mathcal{L}} \approx 1 - \frac{\nu}{2} \exp(-4R\tau), \quad \tau \gg 1.$$

For $\tau \gg 1$, the entropic entanglement coefficient grows unboundedly:

$$I_c \sim \ln(g_1 g_3) \sim 4R\tau.$$

Therefore, in Fig. 4 we compare the compact parameter $\mathcal{J}_c(\tau)$ (58) with the functions $\mathcal{Y}(\tau)$ (17), $\tilde{\mathcal{L}}$ (50), and $[\tilde{\mathcal{L}}(\tau)]^{1/2}$ for the initial vacuum state. Since all formulas, in the asymmetric case, are obtained

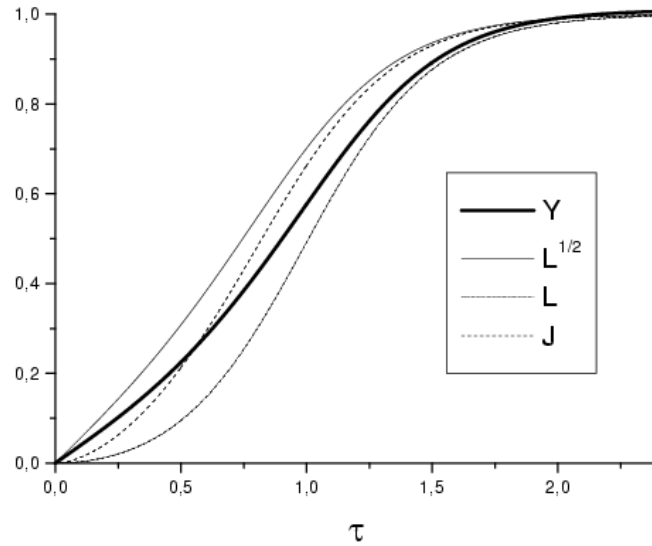


Fig. 4. Time dependences of different entanglement measures under the “asymmetric resonance” condition (62) for $\nu = 100$ and the initial vacuum state. Covariance entanglement coefficient $\mathcal{Y}(\tau)$ (17) is shown by thick line, while thin lines (from bottom to top) exhibit purity entanglement coefficient $\tilde{\mathcal{L}}$ (50), compact entropy entanglement measure $\mathcal{J}_c(\tau)$ (58), and function $[\tilde{\mathcal{L}}(\tau)]^{1/2}$.

neglecting terms of order of ν^{-2} , we use the value $\nu = 100$ in the figures. The difference between the asymptotic values of the functions for $\tau \gg 1$ and the correct value 1 shows the accuracy of approximation ($\sim 2\%$). Dependences of the entanglement covariance and purity coefficients \mathcal{Y} and $\tilde{\mathcal{L}}$ on the “slow time” τ for the initial vacuum and high-temperature states are shown in Fig. 5. Recall that in the high-temperature case the coefficient $\tilde{\mathcal{L}}$ tends to the compact entropic coefficient \mathcal{J}_c .

4. Fabry–Perot Cavity With an Oscillating Boundary

The problem of a scalar massless field in a 1D cavity formed by two infinite ideal plates whose positions are given by

$$x_{\text{left}} \equiv 0$$

and

$$x_{\text{right}} \equiv L(t) = L_0 (1 + \varepsilon \sin [p\omega_1 t]), \quad |\varepsilon| \ll 1, \quad \omega_1 = \frac{\pi c}{L_0}, \quad p = 1, 2, \dots \tag{71}$$

was solved in [45]. The only component of the operator vector potential of the electromagnetic field $\hat{A}(x, t)$ in the Heisenberg representation can be written as

$$\hat{A}(x, t) = \sum_{n=1}^{\infty} \frac{2}{\sqrt{n}} \left[\hat{b}_n \psi^{(n)}(x, t) + \text{h.c.} \right], \quad \left[\hat{b}_n, \hat{b}_k^\dagger \right] = \delta_{nk}, \tag{72}$$

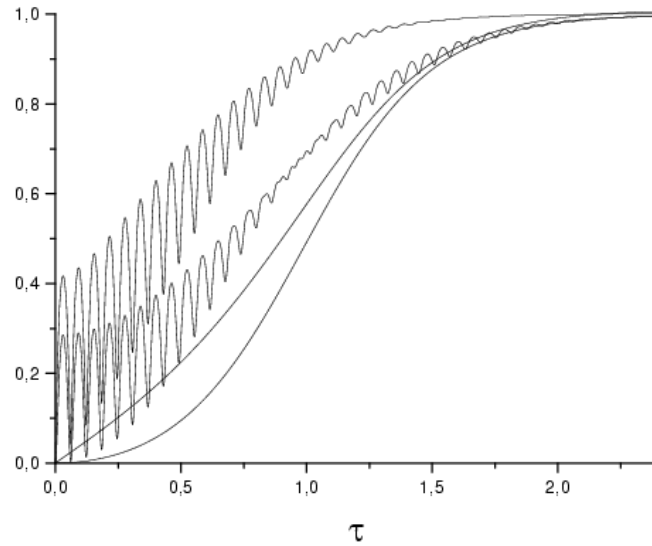


Fig. 5. Covariance entanglement coefficient $\mathcal{Y}(\tau)$ (17) and purity entanglement coefficient $\tilde{\mathcal{L}}(\tau)$ (50) under the “asymmetric resonance” condition (62) for $\nu = 100$ for the initial vacuum state at $\theta_1 = \theta_3 = 1$ (monotonous dependences) and for high-temperature state at $\theta_1 = 3\theta_3$ (oscillating functions). In both cases, upper curves correspond to $\mathcal{Y}(\tau)$ and lower curves correspond to $\tilde{\mathcal{L}}(\tau)$.

where

$$\psi^{(n)}(x, t) = \sqrt{\frac{L_0}{L(t)}} \sum_{k=1}^{\infty} \sin \left[\frac{\pi k x}{L(t)} \right] \left\{ \rho_k^{(n)}(\tau) e^{-i\omega_k t} - \rho_{-k}^{(n)}(\tau) e^{i\omega_k t} \right\}, \tag{73}$$

$$\tau = \frac{1}{2} \varepsilon \omega_1 t, \quad \omega_n = n \omega_1. \tag{74}$$

The normalization factors $2/\sqrt{n}$ in (72) are chosen in such a way that the field energy, in the stationary case, can be represented as the sum of the energies of independent mode oscillators. The coefficients $\rho_k^{(n)}(\tau)$ satisfy an infinite system of coupled equations ($k = \pm 1, \pm 2, \dots; n = 1, 2, \dots$)

$$\frac{d}{d\tau} \rho_k^{(n)} = \sigma \left[(k+p) \rho_{k+p}^{(n)} - (k-p) \rho_{k-p}^{(n)} \right], \quad \sigma \equiv (-1)^p, \tag{75}$$

which was solved in [45] (here we confine ourselves to the simplest special case of solutions found in [45] corresponding to the strict resonance).

Due to the initial conditions

$$\rho_k^{(n)}(0) = \delta_{kn},$$

the solutions to (75) satisfy the relation

$$\rho_{j+mp}^{(k+np)} \equiv 0 \quad \text{if} \quad j \neq k.$$

The nonzero coefficients $\rho_m^{(n)}$ read [45]

$$\rho_{j+mp}^{(j+np)}(\tau) = \frac{\Gamma(1+n+j/p)(\sigma\kappa)^{n-m}}{\Gamma(1+m+j/p)\Gamma(1+n-m)} F(n+j/p, -m-j/p; 1+n-m; \kappa^2), \tag{76}$$

where

$$\kappa = \tanh(p\tau) \tag{77}$$

and $F(a, b; c; z)$ is the Gauss hypergeometric function. The functions (76) are exact solutions to the set of equations (75) relating the coefficients with different lower indices. Besides, these functions satisfy another set of equations, which can be treated as recurrence relations with respect to the upper indices [45]:

$$\frac{d}{d\tau}\rho_m^{(n)} = n \left\{ \sigma \left[\rho_m^{(n-p)} - \rho_m^{(n+p)} \right] \right\}, \quad n \geq p, \quad \rho_m^{(0)} \equiv 0, \tag{78}$$

$$\frac{d}{d\tau}\rho_m^{(n)} = n \left\{ \sigma \left[\rho_{-m}^{(p-n)*} - \rho_m^{(p+n)} \right] \right\}, \quad n = 1, 2, \dots, p-1. \tag{79}$$

The consequences of Eqs. (75), (78), and (79) are the following identities:

$$\sum_{m=-\infty}^{\infty} m \rho_m^{(n)*} \rho_m^{(k)} = n \delta_{nk}, \quad n, k = 1, 2, \dots, \tag{80}$$

$$\sum_{n=1}^{\infty} \frac{m}{n} \left[\rho_m^{(n)*} \rho_j^{(n)} - \rho_{-m}^{(n)*} \rho_{-j}^{(n)} \right] = \delta_{mj}, \quad m, j = 1, 2, \dots, \tag{81}$$

$$\sum_{n=1}^{\infty} \frac{1}{n} \left[\rho_m^{(n)*} \rho_{-j}^{(n)} - \rho_j^{(n)*} \rho_{-m}^{(n)} \right] = 0, \quad m, j = 1, 2, \dots \tag{82}$$

We suppose that after some time T the wall comes back to its initial position L_0 . For $t \geq T$, the field operator assumes the form

$$\hat{A}(x, t) = \sum_{n=1}^{\infty} \frac{2}{\sqrt{n}} \sin(\pi nx/L_0) \left[\hat{a}_n e^{-i\omega_n t} + \text{h.c.} \right], \tag{83}$$

where operators \hat{a}_m are related to the initial operators \hat{b}_n and \hat{b}_n^\dagger by means of the Bogoliubov transformation ($\tau_T \equiv \frac{1}{2}\varepsilon\omega_1 T$)

$$\hat{a}_m = \sum_{n=1}^{\infty} \sqrt{\frac{m}{n}} \left[\hat{b}_n \rho_m^{(n)}(\tau_T) - \hat{b}_n^\dagger \rho_{-m}^{(n)*}(\tau_T) \right], \quad m = 1, 2, \dots \tag{84}$$

The commutation relations

$$\left[\hat{a}_n, \hat{a}_k^\dagger \right] = \delta_{nk}$$

hold due to the identities (80)–(82) which are nothing but the unitarity conditions of the transformation (84). These commutation relations along with the expression for the field energy

$$\hat{H} \equiv \frac{1}{8\pi} \int_0^{L_0} dx \left[\left(\frac{\partial \hat{A}}{\partial t} \right)^2 + \left(\frac{\partial \hat{A}}{\partial x} \right)^2 \right] = \sum_{n=1}^{\infty} \omega_n \left(\hat{a}_n^\dagger \hat{a}_n + \frac{1}{2} \right) \tag{85}$$

convince one that \hat{a}_n and \hat{a}_n^\dagger are true photon annihilation and creation operators at $t \geq T$ (like the operators \hat{b}_n and \hat{b}_n^\dagger are “physical” ones at $t < 0$).

4.1. Intermode Entanglement in the Parametric Resonance Case ($p = 2$)

Our first goal is to calculate the entanglement coefficients between different modes in the case of parametric resonance ($p = 2$). If the initial field state was the vacuum one with respect to the initial operators \hat{b}_n

$$\hat{b}_n|0\rangle = 0$$

(we use here the Heisenberg picture), then the covariance entanglement coefficient between the r th and s th modes is

$$\mathcal{Y}_{r,s} = \left[\frac{|\langle \hat{a}_r \hat{a}_s \rangle|^2 + |\langle \hat{a}_r^\dagger \hat{a}_s \rangle|^2}{2 \left(\langle \hat{a}_r^\dagger \hat{a}_r \rangle + 1/2 \right) \left(\langle \hat{a}_s^\dagger \hat{a}_s \rangle + 1/2 \right)} \right]^{1/2}. \tag{86}$$

Using (84) one can express the average values contained in formula (86) as follows (assuming hereafter $\omega_1 = 1$):

$$\langle \hat{a}_r \hat{a}_s \rangle = -\sqrt{rs} \sum_{n=1}^{\infty} \frac{1}{n} \rho_r^{(n)} \rho_{-s}^{(n)*} = -\sqrt{rs} \sum_{n=1}^{\infty} \frac{1}{n} \rho_s^{(n)} \rho_{-r}^{(n)*}, \tag{87}$$

$$\langle \hat{a}_r^\dagger \hat{a}_s \rangle = \sqrt{rs} \sum_{n=1}^{\infty} \frac{1}{n} \rho_{-r}^{(n)} \rho_{-s}^{(n)*}, \quad \langle \hat{a}_r^\dagger \hat{a}_r \rangle = r \sum_{n=1}^{\infty} \frac{1}{n} \left| \rho_{-r}^{(n)} \right|^2, \tag{88}$$

where the coefficients $\rho_{\pm m}^{(n)}$ should be taken at the time moment T and thus their argument is τ_T . Strictly speaking, expressions (87) and (88) have physical meanings at those time moments T when the wall returns to its initial position, i.e., for $T = N\pi/p$ with an integer N . Consequently, the argument τ_T of the coefficients $\rho_{\pm m}^{(n)}$ in (87) and (88) assumes discrete values

$$\tau^{(N)} = \frac{N\varepsilon\pi}{2p}.$$

One should have in mind, however, that an interesting situation takes place in our problem for the values $\tau \sim 1$ (or larger). Then $N \sim \varepsilon^{-1} \gg 1$ and the minimum increment $\Delta\tau \sim \varepsilon$ is so small that τ_T can be considered as a continuous variable (under the realistic conditions $\varepsilon \leq 10^{-8}$ [16]). For this reason, we omit hereafter the subscript T , writing simply τ instead of τ_T or $\tau^{(N)}$.

Differentiating the right-hand sides of Eqs. (87) and (88) with respect to the “slow time” τ , one can remove the fraction $1/n$ with the aid of recurrence relations (78) and (79). After that, replacing if necessary the summation index n by $n \pm p$, one can verify that almost all terms on the right-hand sides are cancelled and the infinite series are reduced to finite sums. For $p = 2$, we obtain the equations [taking into account that all functions $\rho_m^{(n)}$ are real in the strict resonance case, according to Eq. (76)]

$$\frac{d}{d\tau} \langle \hat{a}_r \hat{a}_s \rangle = -\sqrt{rs} \left[\rho_r^{(1)} \rho_s^{(1)} + \rho_{-r}^{(1)} \rho_{-s}^{(1)} \right], \tag{89}$$

$$\frac{d \langle \hat{a}_r^\dagger \hat{a}_s \rangle}{d\tau} = \sqrt{rs} \left[\rho_r^{(1)} \rho_{-s}^{(1)} + \rho_{-r}^{(1)} \rho_s^{(1)} \right], \quad \frac{d \langle \hat{a}_r^\dagger \hat{a}_r \rangle}{d\tau} = 2r \rho_r^{(1)} \rho_{-r}^{(1)}. \tag{90}$$

For $p = 2$, only odd modes can be excited from the initial vacuum state. In this case, the hypergeometric functions in formula (76) for coefficients $\rho_r^{(n)}$ with $j = 1$ are reduced to some combinations of

complete elliptic integrals of the first and second kinds [45]:

$$\mathbf{K}(\kappa) = \int_0^{\pi/2} \frac{d\alpha}{\sqrt{1 - \kappa^2 \sin^2 \alpha}} = \frac{\pi}{2} F\left(\frac{1}{2}, \frac{1}{2}; 1; \kappa^2\right),$$

$$\mathbf{E}(\kappa) = \int_0^{\pi/2} d\alpha \sqrt{1 - \kappa^2 \sin^2 \alpha} = \frac{\pi}{2} F\left(-\frac{1}{2}, \frac{1}{2}; 1; \kappa^2\right),$$

so that Eqs. (89) and (90) can be integrated for any values of r and s (see [45, 46] or Appendix B for technical details). In particular, for the first few modes we find

$$\langle \hat{a}_1^2 \rangle = \frac{2}{\pi^2 \kappa} [\tilde{\kappa}^2 \mathbf{K}^2 - 2\mathbf{E}\mathbf{K} + \mathbf{E}^2], \quad (91)$$

$$\langle \hat{a}_3^2 \rangle = \frac{2}{9\pi^2 \kappa^3} [\tilde{\kappa}^2(4 - \kappa^2)\mathbf{K}^2 - 2(2\kappa^4 - 3\kappa^2 + 4)\mathbf{E}\mathbf{K} + (4\kappa^4 - \kappa^2 + 4)\mathbf{E}^2], \quad (92)$$

$$\langle \hat{a}_1 \hat{a}_3 \rangle = -\frac{2\sqrt{3}}{3\pi^2 \kappa^2} [\tilde{\kappa}^2 \mathbf{K}^2 - 2\mathbf{E}\mathbf{K} + (1 + \kappa^2)\mathbf{E}^2], \quad (93)$$

$$\langle \hat{a}_1^\dagger \hat{a}_3 \rangle = \frac{2\sqrt{3}}{\pi^2 \kappa} \left[\frac{\tilde{\kappa}^2}{3} \mathbf{K}^2 + \frac{2}{3}(\kappa^2 - 2)\mathbf{E}\mathbf{K} + \mathbf{E}^2 \right], \quad (94)$$

$$\langle \hat{a}_1 \hat{a}_5 \rangle = \frac{2\sqrt{5}}{45\pi^2 \kappa^3} [\tilde{\kappa}^2(\kappa^2 + 8)\mathbf{K}^2 - 2(\kappa^4 + 8)\mathbf{E}\mathbf{K} + (8\kappa^4 + 7\kappa^2 + 8)\mathbf{E}^2], \quad (95)$$

$$\langle \hat{a}_1^\dagger \hat{a}_5 \rangle = -\frac{2\sqrt{5}}{3\pi^2 \kappa^2} \left[\frac{\tilde{\kappa}^2}{5}(2\kappa^2 + 1)\mathbf{K}^2 + \frac{2}{5}(2\kappa^4 - 2\kappa^2 - 3)\mathbf{E}\mathbf{K} + (\kappa^2 + 1)\mathbf{E}^2 \right], \quad (96)$$

$$\langle \hat{a}_3 \hat{a}_5 \rangle = \frac{2\sqrt{15}}{45\pi^2 \kappa^4} [\tilde{\kappa}^2(\kappa^2 + 2)(\kappa^2 - 2)\mathbf{K}^2 + 2(2\kappa^6 - \kappa^4 - 2\kappa^2 + 4)\mathbf{E}\mathbf{K} - 4(\kappa^2 + 1)(\kappa^4 - \kappa^2 + 1)\mathbf{E}^2], \quad (97)$$

$$\langle \hat{a}_3^\dagger \hat{a}_5 \rangle = \frac{2\sqrt{15}}{45\pi^2 \kappa^3} [\tilde{\kappa}^2(7\kappa^2 - 4)\mathbf{K}^2 + 2(8\kappa^4 - 15\kappa^2 + 4)\mathbf{E}\mathbf{K} - (4\kappa^4 - 19\kappa^2 + 4)\mathbf{E}^2], \quad (98)$$

$$\mathcal{E}_1 = \frac{2}{\pi^2} \mathbf{K} (2\mathbf{E} - \tilde{\kappa}^2 \mathbf{K}), \quad (99)$$

$$\mathcal{E}_3 = \frac{2}{3\pi^2 \kappa^2} [(3\kappa^2 - 2)\mathbf{K} (2\mathbf{E} - \tilde{\kappa}^2 \mathbf{K}) + 2(1 + \kappa^2)\mathbf{E}^2] \quad (100)$$

$$\mathcal{E}_5 = -\frac{2}{45\pi^2 \kappa^4} [\tilde{\kappa}^2(47\kappa^4 - 30\kappa^2 - 8)\mathbf{K}^2 + 2(4\kappa^6 - 47\kappa^4 + 26\kappa^2 + 8)\mathbf{E}\mathbf{K} - 2(\kappa^2 + 1)(4\kappa^4 + 11\kappa^2 + 4)\mathbf{E}^2], \quad (101)$$

where

$$\tilde{\kappa} \equiv \sqrt{1 - \kappa^2}$$

and we used

$$\mathcal{E}_r = \langle \hat{a}_r^\dagger \hat{a}_r \rangle + \frac{1}{2}.$$

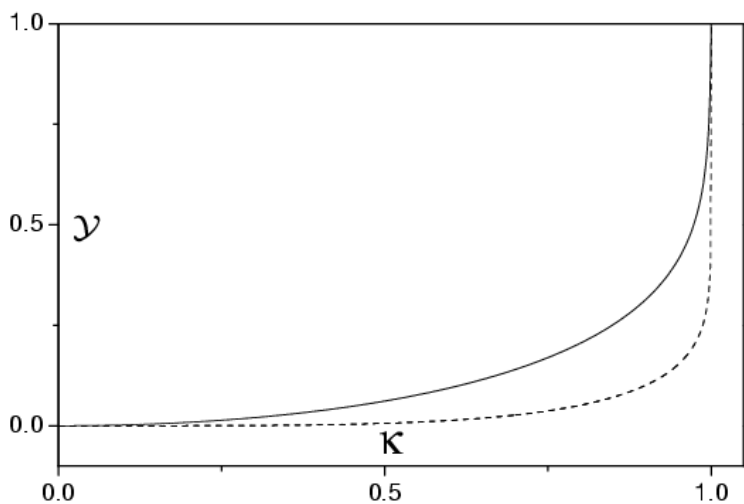


Fig. 6. Covariance entanglement coefficient $\mathcal{Y}_{n,m}$ (86) in the 1D resonance ($p = 2$) cavity versus the compact parameter $\kappa = \tanh(2\tau)$ for the vacuum initial state. $\mathcal{Y}_{1,3}$ (solid curve) and $\mathcal{Y}_{3,5}$ (dash curve).

Functions $\mathcal{Y}_{1,3}$ and $\mathcal{Y}_{3,5}$ are shown in Fig. 6. We see that the entanglement is strongest for the lowest modes. However, for any pair r, s , the coefficient \mathcal{Y}_{rs} tends asymptotically to the unit value at $\kappa \rightarrow 1$. To prove this property, one should use the asymptotic forms of the coefficients $\rho_m^{(n)}$ for $\tau \rightarrow \infty$, i.e., for $\kappa \rightarrow 1$. Namely, by replacing the hypergeometric functions in (76) by their values for the unit argument [47]

$$F(a, b; a + b + 1; 1) = \frac{\Gamma(a + b + 1)}{\Gamma(a + 1)\Gamma(b + 1)},$$

one obtains the following asymptotic formulas (see also [46]):

$$\rho_{2m+1}^{(1)}(\tau) = \rho_{-2m-1}^{(1)}(\tau) = \frac{2(-1)^m}{\pi(2m + 1)}, \quad \tau \rightarrow \infty. \tag{102}$$

Consequently, for $\tau \gg 1$ we have

$$\langle \hat{a}_r^\dagger \hat{a}_s \rangle \approx -\langle \hat{a}_r \hat{a}_s \rangle \approx \frac{8\tau}{\pi^2 \sqrt{rs}} (-1)^{(r-s)/2} + \mathcal{O}(1) \tag{103}$$

and the leading terms in the numerator and denominator of the fraction in (86) become the same for $\tau \rightarrow \infty$.

In the case of detuning from the strict resonance, characterized by some dimensionless detuning parameter γ , the coefficients $\rho_m^{(n)}$ become complex. However, their asymptotic forms differ from (102) only by some phase factors [46]. Since the covariance entanglement coefficient (86) depends on the absolute values of the second-order moments $\langle \hat{a}_r^\dagger \hat{a}_s \rangle$ and $\langle \hat{a}_r \hat{a}_s \rangle$, these phase factors do not influence the

final result, namely, that $\mathcal{Y}_{rs} \rightarrow 1$ when $\tau \rightarrow \infty$, unless the dimensionless detuning parameter exceeds the critical value $\gamma = 1$, when the generation of photons from vacuum becomes impossible.

For the initial vacuum state, the field state at the subsequent moments of time remains Gaussian [46] and the purity entanglement coefficient can be calculated by means of formula (8). In the generic case, the determinant of the symmetrical 4×4 matrix Q (25) contains 17 different terms. However, in the specific case involved all covariances between the “coordinate” and “momenta” operators turn out to be equal to zero identically

$$\widetilde{x_k p_j} = 0,$$

and for this reason the determinant of the covariance matrix for the i th and j th modes can be factorized in the following simple form:

$$\det Q = \left(\sigma_{p_i p_i} \sigma_{p_j p_j} - \sigma_{p_i p_j}^2 \right) \left(\sigma_{x_i x_i} \sigma_{x_j x_j} - \sigma_{x_i x_j}^2 \right). \quad (104)$$

Nonzero covariances are given by the following expressions:

$$\sigma_{x_i x_j} \equiv \overline{x_i x_j} = \frac{1}{2} \langle \hat{a}_i^\dagger \hat{a}_j + \hat{a}_j^\dagger \hat{a}_i \rangle + \text{Re} \langle \hat{a}_i \hat{a}_j \rangle, \quad \sigma_{p_i p_j} \equiv \overline{p_i p_j} = \frac{1}{2} \langle \hat{a}_i^\dagger \hat{a}_j + \hat{a}_j^\dagger \hat{a}_i \rangle - \text{Re} \langle \hat{a}_i \hat{a}_j \rangle. \quad (105)$$

Introducing the correlation coefficients

$$r_{x_i x_j} = \frac{\sigma_{x_i x_j}}{\sqrt{\sigma_{x_i x_i} \sigma_{x_j x_j}}}, \quad r_{p_i p_j} = \frac{\sigma_{p_i p_j}}{\sqrt{\sigma_{p_i p_i} \sigma_{p_j p_j}}}, \quad (106)$$

we can represent the $\tilde{\mathcal{L}}$ (8) and \mathcal{Z} (16) entanglement coefficients between the i th and j th modes as follows

$$\tilde{\mathcal{L}}_{ij} = 1 - \sqrt{\left(1 - r_{x_i x_j}^2\right) \left(1 - r_{p_i p_j}^2\right)}, \quad (107)$$

$$\mathcal{Z}_{ij} = 1 + \sqrt{\left(1 - r_{x_i x_j}^2\right) \left(1 - r_{p_i p_j}^2\right)} - 2 \sqrt{\frac{\left(1 - r_{x_i x_j}^2\right) \left(1 - r_{p_i p_j}^2\right)}{\left(1 - \frac{1}{4} r_{x_i x_j}^2\right) \left(1 - \frac{1}{4} r_{p_i p_j}^2\right)}}. \quad (108)$$

If all correlation coefficients are small (in particular, if $\tau \ll 1$), then

$$\tilde{\mathcal{L}}_{ij} \approx 2\mathcal{Z}_{ij} \approx \frac{1}{2} \left(r_{x_i x_j}^2 + r_{p_i p_j}^2 \right).$$

When $\tau \rightarrow \infty$, then due to Eqs. (103), (105), and (106) the coefficients $\sigma_{p_i p_j}$ grow linearly with time in such a way that the momentum correlation coefficient $r_{p_i p_j}$ tends to the unit value. At the same time, the coefficients $\sigma_{x_i x_j}$ and $r_{x_i x_j}$ tend to some finite limit values. Therefore, the purity entanglement coefficient $\tilde{\mathcal{L}}$ and the distance entanglement coefficient \mathcal{Z} approach the unit value. Using the asymptotic formulas for the complete elliptic integrals [47]

$$\mathbf{K}(\kappa) \approx \ln \frac{4}{\tilde{\kappa}} + \frac{1}{4} \left(\ln \frac{4}{\tilde{\kappa}} - 1 \right) \tilde{\kappa}^2 + \dots, \quad \mathbf{E}(\kappa) \approx 1 + \frac{1}{2} \left(\ln \frac{4}{\tilde{\kappa}} - \frac{1}{2} \right) \tilde{\kappa}^2 + \dots, \quad \kappa \rightarrow 1,$$

one can see that for $\tau \gg 1$

$$1 - \tilde{\mathcal{L}} \sim 1 - \mathcal{Z} \sim \tau^{-1/2}.$$

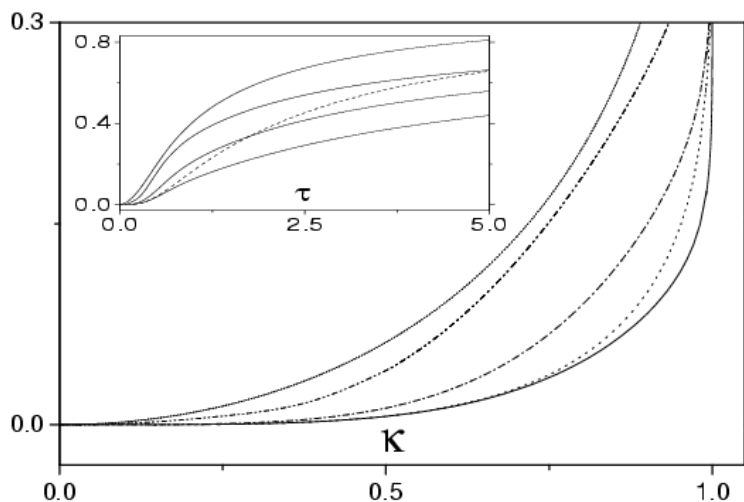


Fig. 7. Different coefficients characterizing entanglement between the first and third modes in the 1D resonance ($p = 2$) cavity versus “slow time” τ (in the insertion) and the compact parameter $\kappa = \tanh(2\tau)$ for the vacuum initial state. The main figure (from top to bottom) show covariance entanglement coefficient \mathcal{Y} (47), compact entropy coefficient \mathcal{J}_c (58), purity entanglement coefficient $\tilde{\mathcal{L}}$ (50), the square of covariance entanglement coefficient \mathcal{Y}^2 (dash curve in the insertion), and distance entanglement coefficient \mathcal{Z} (16).

In particular,

$$1 - \tilde{\mathcal{L}}_{13} \sim \sqrt{\frac{44}{57\tau}} \approx \frac{0.88}{\sqrt{\tau}}, \quad 1 - \mathcal{Z}_{13} \sim \sqrt{\frac{44}{3\tau}} \left(\frac{8}{\sqrt{219}} - \frac{1}{\sqrt{19}} \right) \approx \frac{1.19}{\sqrt{\tau}}.$$

Calculating the entropy entanglement measure (1), one should take into account that the reduced entropy of any two-mode subsystem depends on time in the case involved (in contradiction to the case considered in the previous section) because the evolution of each finite-dimensional subsystem is not unitary. This entropy is determined by two eigenvalues of the corresponding 4×4 matrix $\mathcal{Q}\Omega^{-1}$, which are given by formula (26). The reduced entropy of the k th mode is determined by the single number

$$f_k = \sqrt{\sigma_{p_k p_k} \sigma_{x_k x_k}}, \tag{109}$$

as soon as the coordinate–momentum covariances are equal to zero in the strict resonance case under consideration. The explicit formula for the entropy entanglement measure between the k th and n th modes becomes (for the initial vacuum state of the field)

$$I_c^{kn} = \sum_{j=k,n} \left[(f_j + 1/2) \ln (f_j + 1/2) - (f_j - 1/2) \ln (f_j - 1/2) \right] - \sum_{\delta=\pm 1} \left[\left(f_{kn}^\delta + 1/2 \right) \ln \left(f_{kn}^\delta + 1/2 \right) - \left(f_{kn}^\delta - 1/2 \right) \ln \left(f_{kn}^\delta - 1/2 \right) \right], \tag{110}$$

where

$$2f_{kn}^{\delta} = \left[\overline{p_k p_k} \overline{x_k x_k} + \overline{p_n p_n} \overline{x_n x_n} + 2\overline{p_k p_n} \overline{x_k x_n} + 2\sqrt{(\overline{p_k p_k} \overline{p_n p_n} - \overline{p_k p_n}^2)(\overline{x_k x_k} \overline{x_n x_n} - \overline{x_k x_n}^2)} \right]^{1/2} \\ + \delta \left[\overline{p_k p_k} \overline{x_k x_k} + \overline{p_n p_n} \overline{x_n x_n} + 2\overline{p_k p_n} \overline{x_k x_n} - 2\sqrt{(\overline{p_k p_k} \overline{p_n p_n} - \overline{p_k p_n}^2)(\overline{x_k x_k} \overline{x_n x_n} - \overline{x_k x_n}^2)} \right]^{1/2}. \quad (111)$$

The behavior of different entanglement coefficients is shown in Fig. 7. All of them monotonously tend to unity in the course of time but much more slowly than in the case of asymmetric resonance in the 3D cavity (due to the interaction with other resonant modes).

4.2. Entanglement in the “Semi-Resonance Case” ($p = 1$)

A qualitatively different behavior of all field characteristics is observed in the “semi-resonance case” where the frequency of the boundary oscillations coincides with the fundamental field eigenfrequency ($p = 1$) [45, 48]. In this case, one should put $j = 0$ in formula (76) and all coefficients $\rho_m^{(n)}$ with negative lower indices m are identically equal to zero. As a consequence, no photons can be created from the initial vacuum state, which is clearly seen from Eq. (88). If initially the field was in a nonvacuum state (at least for some mode), then the total number of photons in all modes is conserved, although the total energy grows exponentially due to “heating” of the high-frequency modes (at the expense of “cooling” the low-frequency modes).

We suppose that initially only the first mode was excited, while all the others were in the vacuum state. Then the dynamics of all modes is described by means of the unique coefficient

$$\rho_m^{(1)} = \frac{(\tanh \tau)^{m-1}}{\cosh^2 \tau}.$$

If initially the excited mode was in a coherent state, then all second-order central moments connecting different modes are equal to zero, resulting in the zero covariance entanglement coefficient

$$\mathcal{Y}_{rs}^{\text{coh}} = 0.$$

However, for other initial states we obtain nonzero values of $\mathcal{Y}_{r,s}$.

If initially the first mode was in the Fock state $|n\rangle$, then

$$\mathcal{Y}_{rs}^{\text{Fock}} = \frac{n\zeta_r \zeta_s}{\sqrt{2(n\zeta_r^2 + 1/2)(n\zeta_s^2 + 1/2)}}, \quad (112)$$

where

$$\zeta_m = \sqrt{m} \rho_m^{(1)} = \sqrt{m} \frac{(\tanh \tau)^{m-1}}{\cosh^2 \tau} \leq 1. \quad (113)$$

If initially the first mode was in a squeezed vacuum state

$$|\psi\rangle = \exp \left[\frac{R(\hat{b}_1^{\dagger 2} - \hat{b}_1^2)}{2} \right] |0\rangle$$

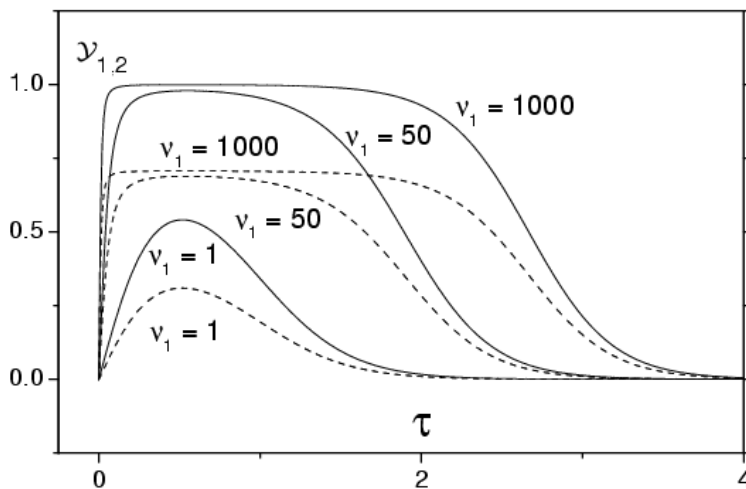


Fig. 8. Covariance entanglement coefficient $\mathcal{Y}_{1,2}$ (86) in the 1D “semi-resonance” ($p = 1$) cavity versus “slow time” τ for the Fock (dash curves) and squeezed vacuum (solid curves) initial states of the first mode with mean photon numbers $\nu_1 = 1, 50, 1000$.

with the mean photon number $\nu_1 = \sinh^2(R)$, then

$$\mathcal{Y}_{rs}^{sqz} = \frac{\zeta_r \zeta_s \sqrt{\nu_1(2\nu_1 + 1)}}{\sqrt{2(\nu_1 \zeta_r^2 + 1/2)(\nu_1 \zeta_s^2 + 1/2)}}. \tag{114}$$

If initially the first mode was in an even/odd coherent state [49]

$$|\alpha_{\pm}\rangle = \frac{|\alpha_1\rangle \pm |-\alpha_1\rangle}{\sqrt{2[1 \pm \exp(-2|\alpha_1|^2)]}},$$

then the mean photon numbers are given by the formulas

$$\nu_1^{(+)} = |\alpha_1|^2 \tanh(|\alpha_1|^2), \quad \nu_1^{(-)} = |\alpha_1|^2 \coth(|\alpha_1|^2).$$

In both cases, the entanglement coefficient can be written as follows:

$$\mathcal{Y}_{rs}^{ev/od} = \frac{\zeta_r \zeta_s \sqrt{\nu_1(\nu_1 + |\alpha_1|^2)}}{\sqrt{2(\nu_1 \zeta_r^2 + 1/2)(\nu_1 \zeta_s^2 + 1/2)}}. \tag{115}$$

For a large enough number of photons in the initial squeezed and even/odd coherent states $\nu_1 \gg 1$, the entanglement coefficient becomes very close to the maximum possible unit value if $\nu_1 \zeta_{r,s}^2 \gg 1$, but with increase of time \mathcal{Y} eventually goes to zero because $\zeta_{r,s}(\tau) \rightarrow 0$ for $\tau \rightarrow \infty$. In the case of the initial Fock state, the maximum value of \mathcal{Y} does not exceed $1/\sqrt{2}$. A typical behavior of the covariance entanglement

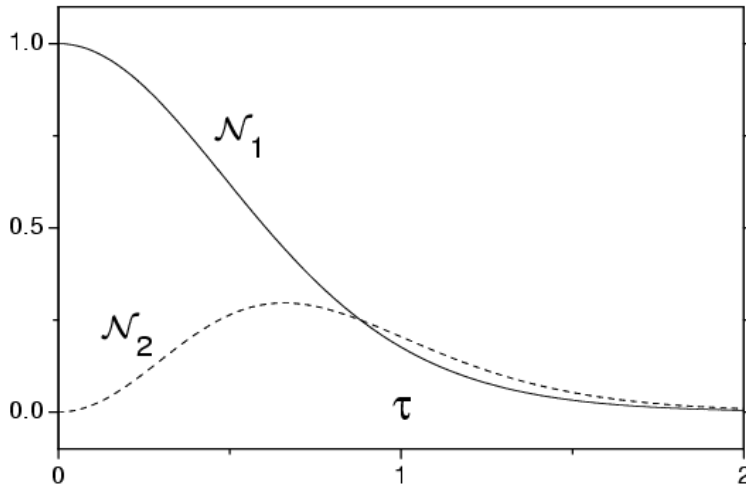


Fig. 9. Mean photon number in the first and second modes of the 1D “semi-resonance” ($p = 1$) cavity versus “slow time” τ for the initial Fock state $|1\rangle$.

coefficient between the first and second modes for the initial Fock and squeezed states is shown in Fig. 8. The behavior of $\mathcal{Y}_{m,n}$ for the initial thermal and even/odd states is very similar, especially for large mean photon numbers. The evolution of the mean photon numbers in the first and second modes is shown in Fig. 9.

The momentum–coordinate covariances turn out to be equal to zero again (as in the case $p = 2$); therefore, we need only two correlation coefficients defined in (106) in order to calculate the purity and distance entanglement coefficients (in the case of the initial squeezed state of the first mode) with the aid of Eqs. (107) and (108). These correlation coefficients are as follows:

$$r_{x_i x_j} = \frac{\chi \zeta_i(\tau) \zeta_j(\tau)}{\sqrt{[1 + \chi \zeta_i^2(\tau)] [1 + \chi \zeta_j^2(\tau)]}}, \quad r_{p_i p_j} = - \frac{\lambda \zeta_i(\tau) \zeta_j(\tau)}{\sqrt{[1 - \lambda \zeta_i^2(\tau)] [1 - \lambda \zeta_j^2(\tau)]}}, \quad (116)$$

where

$$\chi = e^{2R} - 1, \quad \lambda = 1 - e^{-2R}.$$

The time dependences of the $\tilde{\mathcal{L}}$ and \mathcal{Z} entanglement coefficients are compared in Fig. 10. We see that the solid and dash curves are very close, especially for large mean photon numbers.

5. Conclusions

We have compared the time dependences of several functions characterizing the degree of entanglement between field modes of ideal cavities with resonantly vibrating walls for different models of such

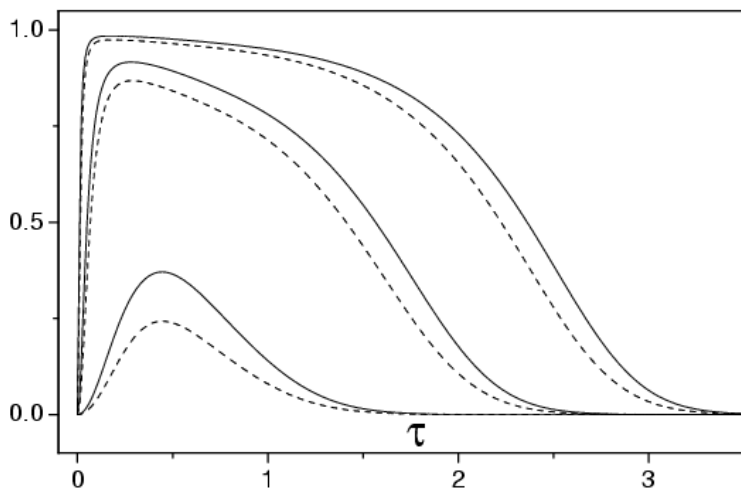


Fig. 10. Purity entanglement coefficient $\tilde{\mathcal{L}}_{1,2}$ (107) (solid curves) and distance entanglement coefficient $\mathcal{Z}_{1,2}$ (108) (dash curves) versus “slow time” τ in the 1D “semi-resonance” ($p = 1$) cavity for the initial squeezed vacuum state of the first mode with different mean photon numbers $\nu_1 = 1, 50, 1000$.

cavities. All these functions (“standard” entropy entanglement measure for Gaussian states, covariance entanglement coefficient introduced in [14, 15], distance entanglement coefficient introduced in [13], and purity entanglement coefficient introduced here) are based on the second-order covariance matrix of the field quadrature components. In spite of having different analytical forms, the coefficients concerned show similar qualitative (and in certain cases even quantitative) behavior for each fixed model. Therefore, the covariance entanglement coefficient, being the simplest one from the viewpoint of calculations, seems to be the most convenient, especially compared with the entropy entanglement measure, whose calculation requires tremendous effort, giving practically the same information on the degree of entanglement. Moreover, the example at the end of Sec. 3.1 shows that the covariance entanglement coefficient (based on traces of covariance submatrices) can be more sensitive to entanglement than other measures (which are based on determinants of covariance submatrices).

On the other hand, the behavior of each selected entanglement coefficient turns out to be completely different for different kinds of cavities. For the three-dimensional cavities with accidental degeneracy of the eigenfrequency spectrum, the entanglement coefficients exhibit oscillations in the case of “symmetric” resonance, remaining relatively small for all instants of time. Moreover, they go to zero periodically, despite the fact that the energy of each mode increases unlimitedly. In the case of “asymmetric” resonance, fast (in the “slow time” scale) oscillations of the entanglement coefficients are also observed, but all these coefficients tend to the maximum possible unit value with increase of time. For the model of a one-dimensional (Fabry–Perot) cavity with equidistant spectrum, all entanglement coefficients monotonously go to the unit value in the parametric resonance case. In the “semi-resonance” case, they rapidly reach values close to unity and remain at this level for some interval of time (which increases with increase in

the initial mean number of quanta) but eventually decay to zero. Therefore, this study adds some new features to our understanding of the behavior of fields in cavities with vibrating boundaries, in addition to the results obtained earlier in [16, 44–46, 50].

Acknowledgment

The authors acknowledge full support of the Brazilian agency CNPq.

Appendix A. Bogoliubov Coefficients in the 1D Parametric Resonance Case

The nonzero coefficients $\rho_{2m+1}^{(1)}$ in the parametric resonance case ($p = 2$) read [45, 46]

$$\rho_{2m+1}^{(1)} = \frac{(-1)^m \Gamma(m+1/2) \kappa^m}{\Gamma(1/2) \Gamma(1+m)} F(m+1/2, -1/2; 1+m; \kappa^2), \quad (\text{A.1})$$

$$\rho_{-2m-1}^{(1)} = \frac{(-1)^m \Gamma(m+1/2) \Gamma(3/2) \kappa^{m+1}}{\pi \Gamma(2+m)} F(m+1/2, 1/2; 2+m; \kappa^2). \quad (\text{A.2})$$

In particular ($\tilde{\kappa} \equiv \sqrt{1-\kappa^2}$),

$$\rho_1^{(1)} = \frac{2}{\pi} \mathbf{E}(\kappa), \quad \rho_{-1}^{(1)} = \frac{2}{\pi \kappa} [\mathbf{E}(\kappa) - \tilde{\kappa}^2 \mathbf{K}(\kappa)], \quad (\text{A.3})$$

$$\rho_3^{(1)} = \frac{2}{3\pi \kappa} [(1-2\kappa^2) \mathbf{E}(\kappa) - \tilde{\kappa}^2 \mathbf{K}(\kappa)], \quad \rho_{-3}^{(1)} = -\frac{2}{3\pi \kappa^2} [(2-\kappa^2) \mathbf{E}(\kappa) - 2\tilde{\kappa}^2 \mathbf{K}(\kappa)], \quad (\text{A.4})$$

$$\rho_5^{(1)} = \frac{2}{15\pi \kappa^2} [(8\kappa^4 - 3\kappa^2 - 2) \mathbf{E}(\kappa) + (-4\kappa^4 + 2\kappa^2 + 2) \mathbf{K}(\kappa)],$$

$$\rho_{-5}^{(1)} = -\frac{2}{15\pi \kappa^3} [(2\kappa^4 + 3\kappa^2 - 8) \mathbf{E}(\kappa) - (\kappa^4 + 7\kappa^2 - 8) \mathbf{K}(\kappa)].$$

The general structure of the coefficients $\rho_{2m+1}^{(1)}$ in terms of the complete elliptic integrals is [46]

$$\rho_{2m+1}^{(1)} = \frac{2}{\pi \kappa^m} [f_m(\kappa^2) \mathbf{E}(\kappa) + \tilde{\kappa}^2 g_m(\kappa^2) \mathbf{K}(\kappa)], \quad (\text{A.5})$$

$$\rho_{-2m-1}^{(1)} = \frac{2}{\pi \kappa^{m+1}} [r_m(\kappa^2) \mathbf{E}(\kappa) + \tilde{\kappa}^2 s_m(\kappa^2) \mathbf{K}(\kappa)], \quad (\text{A.6})$$

where $f_m(x)$, $g_m(x)$, $r_m(x)$, and $s_m(x)$ are polynomials of degree m which can be found from recurrence relations (75).

Appendix B. Calculation of Integrals

To calculate, for instance, the average value $\langle \hat{a}_1^\dagger \hat{a}_3 \rangle$, we use Eqs. (90), (A.3), and (A.4), replacing the derivative over τ by the derivative with respect to κ in accordance with the relation

$$d\kappa = 2\tilde{\kappa}^2 d\tau.$$

In this way, we arrive at the equation

$$\frac{d\langle\hat{a}_1^\dagger\hat{a}_3\rangle}{d\kappa} = -\frac{2\sqrt{3}}{3\pi^2\kappa^2\tilde{\kappa}^2} [(1 + \kappa^2) \mathbf{E}^2(\kappa) - \tilde{\kappa}^4 \mathbf{K}^2(\kappa) - 2\kappa^2\tilde{\kappa}^2 \mathbf{E}(\kappa)\mathbf{K}(\kappa)]. \quad (\text{A.7})$$

Taking into account the differentiation rules [47]

$$\frac{d\mathbf{K}(\kappa)}{d\kappa} = \frac{\mathbf{E}(\kappa)}{\kappa\tilde{\kappa}^2} - \frac{\mathbf{K}(\kappa)}{\kappa}, \quad \frac{d\mathbf{E}(\kappa)}{d\kappa} = \frac{\mathbf{E}(\kappa) - \mathbf{K}(\kappa)}{\kappa}, \quad (\text{A.8})$$

we can suppose that the factor $\tilde{\kappa}^2$ in the denominator on the right-hand side of Eq. (A.7) comes from the derivative $d\mathbf{K}/d\kappa$. Thus it is natural to look for the solution in the form

$$\langle\hat{a}_1^\dagger\hat{a}_3\rangle = \frac{2\sqrt{3}}{3\pi^2\kappa} [A(\kappa)\mathbf{K}^2(\kappa) + B(\kappa)\mathbf{K}(\kappa)\mathbf{E}(\kappa) + C(\kappa)\mathbf{E}^2(\kappa)], \quad (\text{A.9})$$

where $A(\kappa)$, $B(\kappa)$, and $C(\kappa)$ are some polynomials of κ . Putting expression (A.9) into Eq. (A.7) we obtain a set of coupled equations for the coefficients of these polynomials, which can be resolved recursively. The equations for other second-order moments can be integrated in the same manner.

References

1. E. Schrödinger, *Proc. Camb. Phil. Soc.*, **31**, 555 (1935).
2. E. Schrödinger, *Naturwissenschaften*, **23**, 807, 823, 844 (1935) [English translation in: J. A. Wheeler and W. H. Zurek (eds.), *Quantum Theory and Measurement*, Princeton University Press (1983), p. 152].
3. A. Einstein, B. Podolsky, and N. Rosen, *Phys. Rev.*, **47**, 777 (1935).
4. S. M. Barnett and S. J. D. Phoenix, *Phys. Rev. A*, **40**, 2404 (1989); **44**, 535 (1991).
5. A. Mann, B. C. Sanders, and W. J. Munro, *Phys. Rev. A*, **51**, 989 (1995).
6. C. H. Bennett, H. J. Herbert, S. Popescu, and B. Schumacher, *Phys. Rev. A*, **53**, 2046 (1996); S. Popescu and D. Rohrlich, *Phys. Rev. A*, **56**, R3319 (1997); V. Vedral, M. B. Plenio, M. A. Rippin, and P. L. Knight, *Phys. Rev. Lett.*, **78**, 2275 (1997).
7. V. Vedral and M. B. Plenio, *Phys. Rev. A*, **57**, 1619 (1998).
8. W. K. Wootters, *Phys. Rev. Lett.*, **80**, 2245 (1998).
9. M. G. A. Paris, *J. Opt. B: Quantum Semiclass. Opt.*, **1**, 299 (1999); M. J. Donald and M. Horodecki, *Phys. Lett. A*, **264**, 257 (1999); M. Horodecki, P. Horodecki, and R. Horodecki, *Phys. Rev. Lett.*, **84**, 2014 (2000); *Phys. Rev. Lett.*, **84**, 2263 (2000); S. Parker, S. Bose, and M.B. Plenio, *Phys. Rev. A*, **61**, 032305 (2000); T. Hiroshima, *Phys. Rev. A*, **63**, 022305 (2001).
10. R. Horodecki, P. Horodecki, and M. Horodecki, *Phys. Lett. A*, **210**, 377 (1996); K. Zyczkowski, P. Horodecki, A. Sanpera, and M. Lewenstein, *Phys. Rev. A*, **58**, 883 (1998); E. Santos and M. Ferrera, *Phys. Rev. A*, **62**, 024101 (2000); P. Zanardi, C. Zalka, and L. Faoro, *Phys. Rev. A*, **62**, 030301 (2000); W. J. Munro, D. F. V. James, A. G. White, and P. G. Kwiat, *Phys. Rev. A*, **64**, 030302 (2001).
11. K. Furuya, M. C. Nemes, and G. Q. Pellegrino, *Phys. Rev. Lett.*, **80**, 5524 (1998); R. M. Angelo, K. Furuya, M. C. Nemes, and G. Q. Pellegrino, *Phys. Rev. A*, **64**, 043801 (2001); J. Gemmer and G. Mahler, *Euro. Phys. J. D*, **17**, 385 (2001).

12. C. Witte and M. Trucks, *Phys. Lett. A*, **257**, 14 (1999);
M. Ozawa, *Phys. Lett. A*, **268**, 158 (2000).
13. V. I. Man'ko, G. Marmo, E. C. G. Sudarshan, and F. Zaccaria, *J. Phys. A: Math. Gen.*, **35**, 7137 (2002).
14. A. S. M. de Castro and V. V. Dodonov, *J. Russ. Laser Res.*, **23**, 93 (2002).
15. V. V. Dodonov, A. S. M. de Castro, and S. S. Mizrahi, *Phys. Lett. A*, **296**, 73 (2002).
16. V. V. Dodonov and A. B. Klimov, *Phys. Rev. A*, **53**, 2664 (1996).
17. F. R. Gantmakher, *The Theory of Matrices*, Nauka, Moscow (1966).
18. V. Peřinová, A. Lukš, J. Křepelka, C. Sibia, and M. Bertolotti, *J. Mod. Opt.*, **38**, 2429 (1991).
19. V. V. Dodonov, O. V. Man'ko, V. I. Man'ko, and A. Wünsche, *J. Mod. Opt.*, **47**, 633 (2000);
A. Wünsche, V. V. Dodonov, O. V. Man'ko, and V. I. Man'ko, *Fortschr. Phys.*, **49**, 1117 (2001).
20. L.-M. Duan, G. Giedke, J. I. Cirac, and P. Zoller, *Phys. Rev. Lett.*, **84**, 2722 (2000);
R. Simon, *Phys. Rev. Lett.*, **84**, 2726 (2000);
R. F. Werner and M. M. Wolf, *Phys. Rev. Lett.*, **86**, 3658 (2001);
P. Marian, T. A. Marian, and H. Scutaru, *J. Phys. A: Math. Gen.*, **34**, 6969 (2001);
S. Scheel and D.-G. Welsch, *Phys. Rev. A*, **64**, 063811 (2001).
21. V. V. Dodonov and V. I. Man'ko, in: *Group Theory, Gravitation and Elementary Particle Physics, Proceedings of the P. N. Lebedev Physycal Institute*, Nauka, Moscow (1986), Vol. 167, p. 7 [translated by Nova Science, New York (1987), Vol. 167, p. 7].
22. A. Lukš, and V. Peřinová, *Czech. J. Phys.*, **39**, 392 (1989).
23. A. S. Holevo, M. Sohma, and O. Hirota, *Phys. Rev. A*, **59**, 1820 (1999).
24. V. V. Dodonov, in: V. V. Dodonov and V. I. Man'ko (eds.), *Theory of Nonclassical States of Light*, Taylor & Francis, London (in press), p. 153.
25. E. Schrödinger, *Ber. Kgl. Akad. Wiss. Berlin*, **24**, 296 (1930);
H. P. Robertson, *Phys. Rev.*, **35**, 667 (1930).
26. V. V. Dodonov, E. V. Kurmyshev, and V. I. Man'ko, *Phys. Lett. A*, **79**, 150 (1980).
27. V. V. Dodonov and V. I. Man'ko, *Invariants and Evolution of Nonstationary Quantum Systems, Proceedings of the P. N. Lebedev Physycal Institute*, Nova Science, New York (1989), Vol. 183.
28. G. S. Agarwal, *Phys. Rev. A*, **3**, 828 (1971).
29. V. Peřinová, J. Křepelka, J. Peřina, A. Lukš, and P. Szlachetka, *Opt. Acta*, **33**, 15 (1986).
30. V. V. Dodonov, *J. Phys. A: Math. Gen.*, **33**, 7721 (2000);
V. V. Dodonov and O. V. Man'ko, *J. Russ. Laser Res.*, **21**, 438 (2000); *J. Opt. Soc. Am. A*, **17**, 2403 (2000).
31. D. A. Trifonov, *J. Opt. Soc. Am. A*, **17**, 2486 (2000).
32. V. V. Dodonov, in: M. W. Evans (ed.), *Modern Nonlinear Optics, Advances in Chem. Phys. Series*, Wiley, New York (2001), Vol. 119, Pt. 3, p. 309.
33. V. V. Dodonov, A. B. Klimov, and V. I. Man'ko, *Phys. Lett. A*, **142**, 511 (1989).
34. J. Schwinger, *Proc. Nat. Acad. Sci. USA*, **90**, 958 (1993).
35. G. Barton and C. Eberlein, *Ann. Phys. (NY)*, **227**, 222 (1993).
36. A. Lambrecht, M.-T. Jaekel, and S. Reynaud, *Phys. Rev. Lett.*, **77**, 615 (1996).
37. C. K. Law, *Phys. Rev. A*, **49**, 433 (1994); **51**, 2537 (1995).
38. R. Schützhold, G. Plunien, and G. Soff, *Phys. Rev. A*, **57**, 2311 (1998).
39. R. Schützhold, G. Plunien, and G. Soff, *Phys. Rev. A*, **65**, 043820 (2002);
G. Schaller, R. Schützhold, G. Plunien, and G. Soff, *Phys. Rev. A*, **66**, 023812 (2002).

40. H. Saito and H. Hyuga, *Phys. Rev. A*, **65**, 053804 (2002).
41. L. A. S. Machado and P. A. Maia Neto, *Phys. Rev. D*, **65**, 125005 (2002).
42. C. K. Cole and W. C. Schieve, *Phys. Rev. A*, **64**, 023813 (2001).
43. M. Croce, D. A. R. Dalvit, and F. D. Mazzitelli, *Phys. Rev. A*, **64**, 013808 (2001).
44. A. V. Dodonov and V. V. Dodonov, *Phys. Lett. A*, **289**, 291 (2001).
45. V. V. Dodonov, *J. Phys. A: Math. Gen.*, **31**, 9835 (1998).
46. V. V. Dodonov and M. A. Andreata, *J. Phys. A: Math. Gen.*, **32**, 6711 (1999).
47. I. S. Gradshteyn and I. M. Ryzhik, *Tables of Integrals, Series and Products*, Academic Press, New York (1994).
48. V. V. Dodonov, *Phys. Lett. A*, **213**, 219 (1996).
49. V. V. Dodonov, I. A. Malkin, and V. I. Man'ko, *Physica*, **72**, 597 (1974).
50. M. A. Andreata and V. V. Dodonov, *J. Phys. A: Math. Gen.*, **33**, 3209 (2000).